COMPARISON OF THE EXHAUST EMISSIONS FROM A SYNCHRONOUS CHARGE TRAPPING ENGINE AND A ROTAX E-TEC ENGINE

A Thesis

Presented in Partial Fulfillment of the Requirements for the

Degree of Master of Science

with a

Major in Mechanical Engineering

in the

College of Graduate Studies

University of Idaho

by

Alexander Fuhrman

October 2013

Major Professor: Karen Den Braven, Ph.D.

Authorization to Submit Thesis

This thesis of Alexander Fuhrman, submitted for the degree of Master of Science with a major in Mechanical Engineering and titled "COMPARISON OF THE EXHAUST EMISSIONS FROM A SYNCHRONOUS CHARGE TRAPPING ENGINE AND A ROTAX E-TEC ENGINE," has been reviewed in final form. Permission, as indicated by the signatures and dates given below, is now granted to submit final copies to the College of Graduate Studies for approval.

Major Professor _____ Date _____
Karen Den Braven, Ph.D.

Committee Member _____ Date _____
Daniel Cordon, Ph.D.

Committee Member _____ Date _____
David McIlroy, Ph.D.

Department Administrator _____ Date _____
John Crepeau, Ph.D.

Discipline's College Dean _____ Date _____
Larry Stauffer, Ph.D.

Final Approval and Acceptance by the College of Graduate Studies

_____ Date _____
Jie Chen, Ph.D.

Abstract

The University of Idaho has been developing synchronous charge trapping (SCT) two-stroke engines since 2010 for the recreational products industry. Previous testing of SCT engines has shown promise for reduced emissions and fuel consumption, while maintaining performance. The primary goal of this thesis was to complete an EPA 5 Mode emissions test of the parallel rotary synchronous charge trapping (PR-SCT) engine along with defining its maximum performance, as all previous testing had been completed at low load operating points. This research also covers the design, manufacturing, and comparison testing of a new valve design for the PR-SCT. The engine was compared to previous testing results of the PR-SCT along with results from the stock engine on which the PR-SCT is based.

Analysis of the PR-SCT new valve design proved it to be superior to the original valve design surpassing it in every measured parameter, while being equal to the stock engine, within the error of the measurements. During calibration of the engine for the EPA 5-mode test it was discovered that the PR-SCT suffers from incomplete combustion, likely due to excessive amounts of residual exhaust gases (EGR). It was also discovered that major changes in the crank angle at which the valve closes were not needed, except at wide open throttle (WOT). While suffering from inefficient combustion the PR-SCT was still capable of producing 60 Hp and 45 ft-lbs of torque and was able to surpass the stock engine's emissions score.

Acknowledgements

I would like to thank the National Institute for Advanced Transportation Technology (NIATT) for funding my research and making it possible. My Major Professor, Dr. Karen Den Braven, deserves a huge thank you for her guidance on this thesis as well as my undergraduate degree, and her continual devotion to the University of Idaho Clean Snowmobile Challenge Team (UICSC). My committee members Dr. Dan Cordon and Dr. David McIlroy also deserve thanks for their help in reviewing this thesis. I would also like to additionally thank Dr. Dan Cordon for all his insight during the testing and data analysis for this thesis. Russ Porter also deserves thanks for his guidance and help in the manufacturing and assembly of components; without his help it wouldn't have been possible. Thank you to Drew Hooper, Nick Harker, Peter Britanyak, Dylan Dixon, Austin Welch, Sam Smith, Dillon Savage, Rory Lilley, Crystal Green and the 2007 through 2013 UI CSC teams for all of your time, knowledge and devotion to the team and this project. Lastly I would like to thank my parents Miles and Karen Fuhrman and my girlfriend Chandra Logan for your continual support and encouraging me to pursue my master's degree.

Table of Contents

List of Figures

List of Tables

List of Equations

Definition of Terms

m_{tr}	Mass of Trapped Charge
m_{ref}	Mass Reference Charge
m_{tas}	Mass of Trapped Scavenged Charge
m_{ex}	Mass of Retained Exhaust Charge
m_{ar}	Mass of Fresh Air Charge Retained from Previous Cycle
m_{as}	Mass of Charge Scavenged into Cylinder
SR	Scavenging Ratio
SE	Scavenging Efficiency
EC	Exhaust Port Close
EO	Exhaust Port Open
PR-SCT	Parallel Rotary Synchronous Charge Trapping
RAVE	Rotax Adjustable, Variable Exhaust
SCT	Synchronous Charge Trapping
TC	Transfer Port Close
TDC	Top Dead Center
TE	Trapping Efficiency
TO	Transfer Port Open
CE	Charging Efficiency
BMEP	Brake Mean Effective Pressure
BSFC	Brake Specific Fuel Consumption
CO	Carbon Monoxide
HC	Hydrocarbons
NO_x	Nitrogen Oxides
BDC	Bottom Dead Center
BTDC	Before Bottom Dead Center
SAE	Society of Automotive Engineers
CSC	Clean Snowmobile Challenge
TDC	Top Dead Center

1 Introduction

For nearly a decade, the University of Idaho has been working to develop clean two-stroke engine technology primarily for the snowmobile and recreational markets. This work has been driven by the goal to meet or to exceed the goals of the Society of Automotive Engineers (SAE) Clean Snowmobile Challenge (CSC), along with the regulations established by the Environmental Protection Agency (EPA). Since 2010, the University of Idaho has been working to develop viable synchronous charge trapping technology to further improve upon its clean two-stroke engines.

1.0 Research Goals

Performance testing on the University of Idaho Parallel Rotary Synchronous Charge Trapping (PR-SCT) engine has previously only been performed at low operating speeds and low load. The primary goal of this research is to compare the PR-SCT engine with the stock Ski-Doo engine on which it is based, and determine the performance and durability limitations of the current design. Steady state testing of the exhaust emissions, fueling values and power sweeps will be used to compare the engine. This will give the University a better opportunity to market the PR-SCT, as current prospective investors are wary, due to the lack of full emissions and performance testing. Previous testing has shown that the previous valve in the PR-SCT engine has little to no effect. An additional goal of this research will to be to compare testing results of the new valve design, built for this research, to the original valve design.

2 The Two-Stroke Engine

The two-stroke engine is a mechanically simple and low cost engine. The basic moving parts are the piston, connecting rod, and crankshaft. However, while mechanically simple, the fluid flow through the engine is difficult to precisely measure, predict, and model. The major advantage of a two-stroke engine over a four-stroke engine is its high power density, typically at the price of higher exhaust emissions and fuel consumption. This advantage, along with its low production cost, makes the two-stroke engine the preferred choice in the snowmobile industry.

2.0 Two-Stroke Cycle

The two-stroke cycle begins with the piston traveling upwards towards top dead center (TDC). As the piston is traveling upward, it is compressing the fuel air charge in the cylinder. During the compression stroke, a vacuum is formed in the crankcase, pulling in the fresh charge through intake port or reed valve. The charge is then ignited and the piston is forced downwards towards bottom dead center (BDC) as shown in Figure 1. The basics of a two-stroke engine with a tuned pipe will be shown in Figures 1-3 [1].

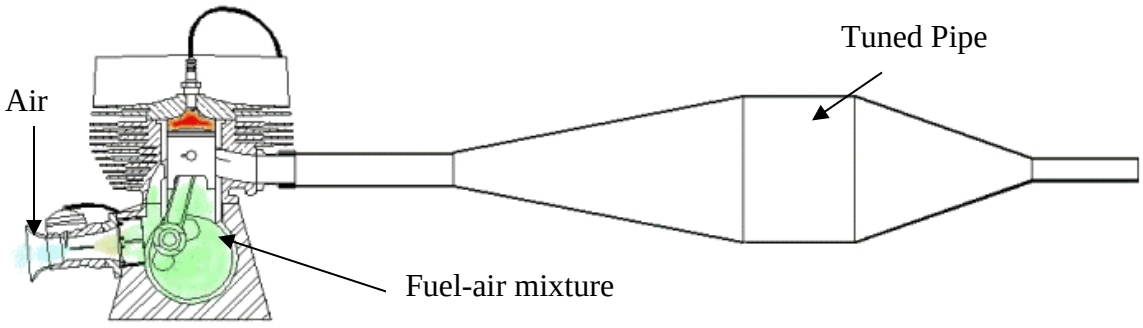

Figure 1: Combustion Process

As the piston travels towards BDC, the exhaust port and transfer ports are uncovered and the scavenging process begins. During this process, the crankcase volume decreases and the transfer or scavenging ports in the cylinder are uncovered.

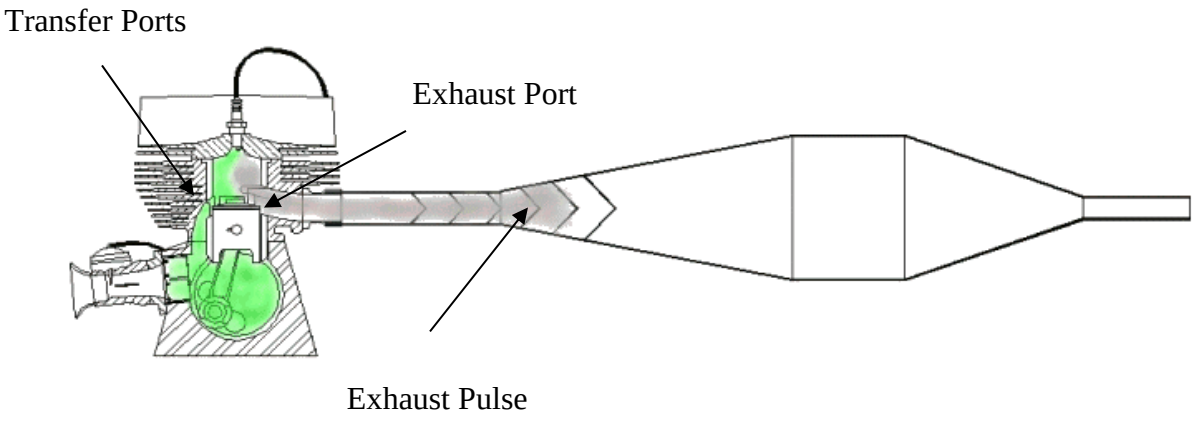

Figure 2: Scavenging Process

When the transfer ports open, the fresh charge begins flowing into the cylinder and scavenges the exhaust gases out of the cylinder as shown in Figure 2. As the piston begins moving upward again, the scavenging process continues and some of the fresh intake charge escapes out of the cylinder.

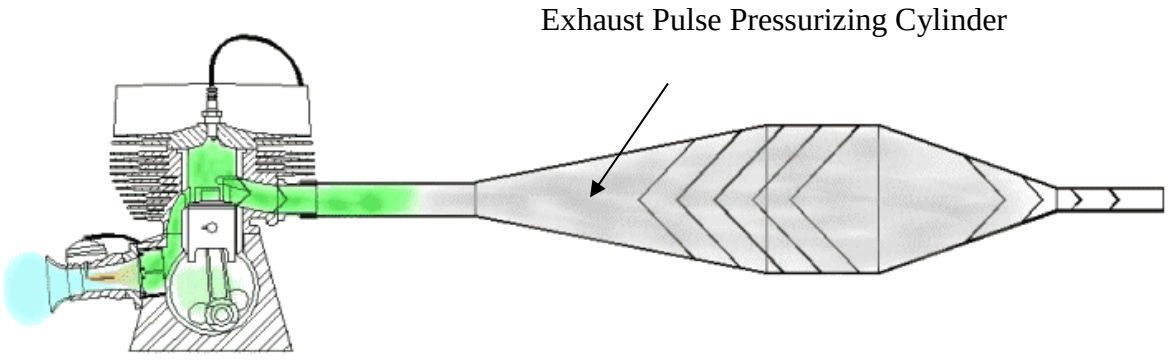

Figure 3: Intake Charge being forced back into cylinder

A method of improving engine performance, in a certain RPM range, is by a tuned exhaust pipe. A tuned exhaust pipe can aid in scavenging and charging of the engine, by creating an oscillating exhaust pulse that helps scavenge exhaust gases (EG) and forces back escaped

intake charge **[2]**. Figure 3 shows escaped charge along with the tuned exhaust pipe wave heading back towards the exhaust port.

2.1 Tuned Exhaust Pipe

A tuned exhaust, or tuned pipe as they are commonly called, uses expansion and compression waves to aid in the scavenging of EG, and also in the retention of intake charge and increased in-cylinder pressure. These effects are caused by pressure waves in the changing area of the tuned pipe. When a positive pressure wave is traveling through an expanding area, or divergent cone, a negative wave is created in the direction of travel, aiding in the scavenging process of EG. This negative wave may also cause the intake charge to be short-circuited; or pulled out of the combustion chamber area, leading to higher emissions. The other effect, caused by an exhaust wave, is when the wave is traveling through a converging area; a positive wave is reflected towards the exhaust port, which forces escaped intake charge back into the cylinder, while boosting in-cylinder pressure. However, while a tuned exhaust can be beneficial, it can also be detrimental. A tuned exhaust is designed to operate within a limited engine speed and EG temperature range. If a tuned exhaust is operating out of these ranges, the negative and positive waves can arrive at incorrect times, leading to lower engine performance and higher emissions. For example, when a compression wave arrives too early, it will pressurize the cylinder; but with the exhaust port not closed, the pressure will be allowed to escape along with the intake charge out of the exhaust, providing little to no increase of in-cylinder pressure, and will increase short circuited fuel. Engine operating points, where the tuned pipe is having detrimental or no positive effect, are commonly referred to as “off the pipe” points or “off- tune” points.

[2] For further explanation on the two-stroke cycle, along with the tuned pipe effect, refer to: [3] [4].

2.2 Direct Fuel Injection

Direct injection involves the use of a specifically designed fuel injector to direct the fuel into the combustion chamber at a specific time. This ability to inject the fuel at a precise time and quantity allows for less fuel to short-circuit out the exhaust of the engine, leading to increased efficiency and decreased exhaust emissions. While direct injection is common to the automotive industry, it is a relatively new concept in the recreational products industry. The University of Idaho has been developing direct injection two-stroke engines since 2003 and successfully implemented it in 2007, with a first place finish at the SAE CSC.

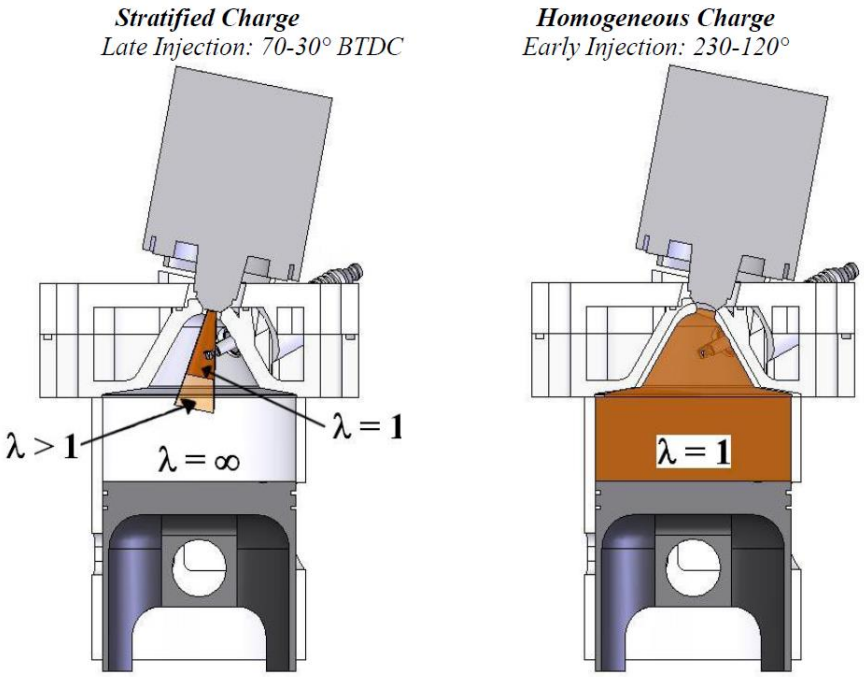

Figure 4: Comparison of Stratified and Homogeneous Intake Charges

A conventional two-stroke engine uses homogeneous combustion, meaning the fuel and air is mixed thoroughly and evenly before ignition. Direct injection is capable of stratified charge combustion. Stratified combustion occurs when fuel is injected extremely late in the cycle and is immediately followed by ignition, which produces a rich flame front around the spark plug, while the rest of the cylinder is globally lean. Stratified combustion is most effective at low engine speed and load, as the reduced mixing time produces less power output. [5] The ability to switch between stratified and homogeneous combustion allows for a direct injection engine to be fuel efficient at low speed and load, while still capable of high power output at high load. A visual example of the difference between stratified and homogeneous charges is shown in Figure 4. For further explanation of direct injection and stratified and homogeneous combustion, see thesis's written at the University of Idaho by Bradbury and Johnson. [6] [5]

2.3 Exhaust Valves

Currently, the method used in the power sports industry to improve engine performance and decrease emissions at off- tune points, is to change the exhaust port height through use of a guillotine-style valve. By raising and lowering the exhaust port height, the point at which the exhaust port is closed and opened can be changed. The valve is kept in a lowered position during low to mid-load, increasing the trapped compression ratio, along with duration of the expansion stroke. By keeping the valve in lowered position during low to mid-load, the change in exhaust port height helps prevent mistimed pressure pulses from the tuned pipe, from causing increased lost intake charge and decreased measured torque. During high load, the valve is pulled up and the exhaust port area is unaffected by the valve. Further explanation and testing of power valves can be seen in Dixon's thesis. [4]

2.4 Synchronous Charge Trapping (SCT)

2.4.1 Reciprocating Synchronous Charge Trapping (R-SCT)

The synchronous charge trapping engine was designed and built in the summer of 2010 by Peter Britanyak. [7] The design was inspired by prototype engines built by Boyesen and Lotus, with the goal of decreasing fuel lost out the exhaust port, and in the case of Lotus, to trap hot residual gases to help initiate homogeneous charge compression ignition (HCCI). Britanyak's design incorporated a hyperbolic shaped valve that used a reciprocating motion to move the valve in the exhaust port area during compression, preventing the intake charge from escaping. During scavenging, the valve would move up and out of the way of the exhaust port. A sectioned view of a rendering of Britanyak's engine is shown in Figure 5.

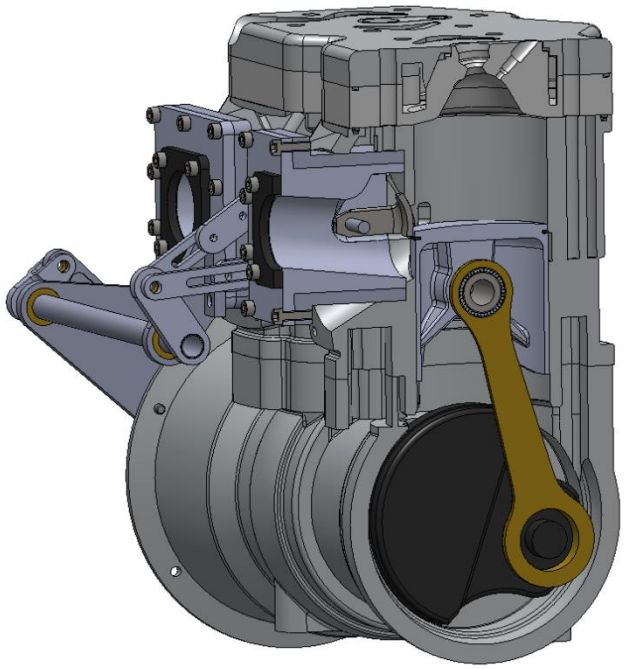

Figure 5: Sectioned view of Britanyak's Reciprocating Synchronous Charge Trapping Engine

Britanyak's engine proved successful in that it achieved a 30% increase in measured torque, while matching stock brake specific fuel consumption (BSFC) and a 10% decrease in BSFC, while matching stock torque at 3500 RPM. [7] Britanyak's work also provided proof of the viability and feasibility of SCT. The reliability of the engine proved to be low, as the reciprocating motion of the valve would cause the valve shaft to shear at 4000 RPM. During the fall of 2010, a student design team looked into redesigning the R-SCT to prevent failure of the valve shaft, but found this to be unachievable within the design constraints of the R-SCT cylinders. [8]

2.4.2 Parallel Rotary Synchronous Charge Trapping (PR-SCT)

The PR-SCT was designed and built during the 2010-2011 school year by four University of Idaho senior engineering students. Initially, the project began as a redesign of R-SCT to improve its survivability, but the project quickly moved to a complete redesign, utilizing a rotary valve motion to decrease forces in the valve shaft. The valve design was similar to that of Britanyak in that they are hyperbolically shaped to match the exhaust port geometry. Additionally, the valves utilized counter weights to balance forces on the valve shaft. The valve position relative to piston position is shown in Figure 6 during the compression stroke on the right, and the scavenging stroke on the left. The valve shaft rotates in the opposite direction of the crankshaft to prevent the valve obstructing gas flow during the scavenging process. For more on the design of the PR-SCT engine, refer to the team's final report. [8]

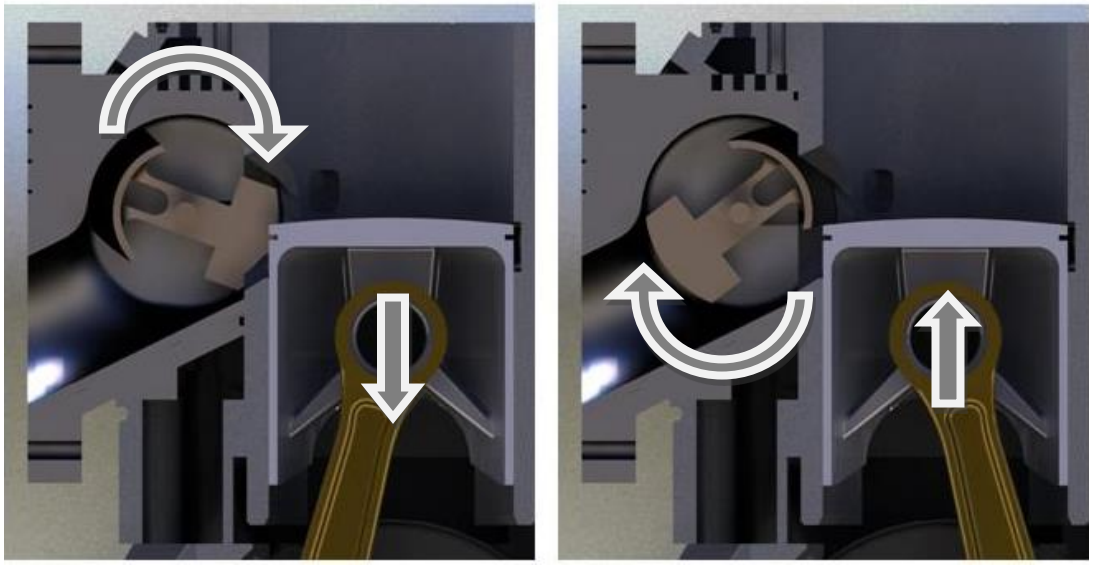

Figure 6: Valve Position during compression and scavenging

2.5 Scavenging Ratio

Scavenging ratio (SR) is the mass of air supplied to the engine during the scavenging process (m_{as}) over the mass that could fill the entire geometric cylinder volume which is represented as the reference mass or (m_{sref}). Scavenging ratio is useful in determining the effectiveness of the scavenging process and determining flow issues. A SR greater than unity, is not uncommon in a two-stroke engine due to the tuned pipe effect. [9]

$$SR = \frac{m_{as}}{m_{sref}}$$

Equation 1: Scavenging Ratio

2.6 Scavenging Efficiency

Scavenging efficiency (SE) is the measure of the effectiveness of an engine in removing exhaust products and pulling in a fresh intake charge. It is defined as the mass of the air delivered that is trapped (m_{tas}) over the total mass charge that is trapped ($m_{tr)}$. The total mass charge is a combination of (m_{tas}), along with the mass of the residual exhaust gases (m_{ex}),

and the mass of any remaining air from the previous cycle (m_{ar}). In theory, a SE equal to the SR is an ideal situation, where all m_{ex} and m_{ar} are removed. Scavenging efficiency is a term worth noting, but for the focus of this research, it will not be considered. The capability to measure m_{ex} and m_{ar} is currently not possible at the U of I. Adding this capability would increase the ability of the facility in determining the flow characteristics of exhaust systems and cylinders.

$$SE = \frac{m_{tas}}{m_{tr}} = \frac{m_{tas}}{m_{tas+m_{ex}+m_{ar}}}$$

Equation 2: Scavenging Efficiency

2.7 Trapping Efficiency

Trapping efficiency (TE) is the ability of the engine to contain the m_{as} and the mass of fuel injected (m_f). One method of determining the trapping efficiency is to measure the trapping efficiency of the air (TE_{air}), which is simply defined as the ratio of m_{tas} over m_{as}. In practice, air trapping efficiency is difficult to simply measure, as m_{tas} is difficult to accurately measure. [9]

$$TE_{air} = \frac{m_{tas}}{m_{as}}$$

Equation 3: Trapping Efficiency

However, it is possible to calculate the TE_{air} using measurements of the exhaust products at specific conditions. If the engine is operating under rich or stoichiometric conditions, and is homogeneously charged, the TE can be calculated as one minus the ratio of the air lost to the exhaust to the air supplied m_{as}.

$$TE_{air} = 1 - \frac{air\ lost\ to\ the\ exhaust}{m_{as}}$$

Equation 4: Trapping Efficiency Air Lost

This equation can then be divided into individual measureable values where (AFR_o) is the overall fuel ratio, ($V\%O_2$) is the percentage volumetric concentration of oxygen; and (MO_2) and (M_{ex}) are the molecular weights of oxygen and the exhaust components. [9]

$$TE_{air} = 1 - \frac{(1 + AFR_o) * V\%O_2 * MO_2}{23.14 * AFR_o * M_{ex}}$$

Equation 5: Trapping Efficiency Exhaust Products

Another method of calculating the air trapping efficiency is ratio of CO, CO_2, NO and O_2, which Douglas defines as Equation 6. In this equation, K_w is the water-gas equilibrium constant times the ratio of (CO_2) over (CO) plus (CO_2). Douglas's equation proves to be the best method for calculating the air trapping efficiency, as it is the most robust method with limited stipulations. [10]

$$TE_{air} = \frac{.5[CO] + [CO_2] + .25 * K_w * \alpha([CO] + [CO_2]) + .5[NO]}{.5[CO] + [CO_2] + [O_2] + .5 * K_w * \alpha([CO] + [CO_2]) + .25[NO]}$$

Equation 6: Air Trapping Efficiency Suggested by Douglas

Another method of calculating TE is by measuring the fuel trapping efficiency TE_{fuel}, which Douglas defines as Equation 7. Fuel trapping efficiency provides the best measure for determining trapping performance, as it has no stipulations as to when it can be applied and was for comparison of TE in this thesis. [10]

$$TE_{fuel} = \frac{[CO] + [CO_2]}{[CO] + [CO_2] + [HC]}$$

Equation 7: Fuel Trapping Efficiency

2.8 Charging Efficiency

Charging efficiency is the ratio of m_{tas} over (m_{sref}). It is a measure of the effectiveness of filling and trapping the cylinder with a fresh air charge. Charging efficiency can also be defined as the product of TE and SR. For the purpose of this research, charging efficiency will not be considered as the measure of trapping efficiency is not certain. Measuring the mass of the fresh air charge trapped is not a capability at the U of I, but should be added with future improvements.

$$CE = \frac{m_{tas}}{m_{sref}} = TE * SR$$

Equation 8: Charging Efficiency

3 Parallel Rotary Synchronous Charge Trapping Remodel

The PR-SCT continues to develop and expose strengths and weaknesses in its design with every round of testing. The PR-SCT has steadily improved with each iteration of development, but continues to suffer from issues involving its belt drive and valve assemblies.

3.0 Belt Drive Remodel

The belt drive system has been a consistent issue for the PR-SCT, since it was built in 2011. Past belt drive systems have suffered from inconsistent belt tension, bearing failure, oscillating valve speeds, and difficulty in adjustment of the valve's position relative to the crankshaft. The most recent iteration, by Hooper, provided a simple solution that negated bearing failure in the idler pulleys, oscillating valve speed issues, and made valve position adjustment relatively simple. [3] While simple to adjust, the movement of Hooper's system was not linear, was limited to only 10 degrees change in valve advancement, and had no possibility of retarding valve timing. The limitations of this system were discovered during the assembly of the engine prior to testing, and eliminated the possibility of a redesign due to time restrictions. The current belt design as built is shown in Figure 7. [3]

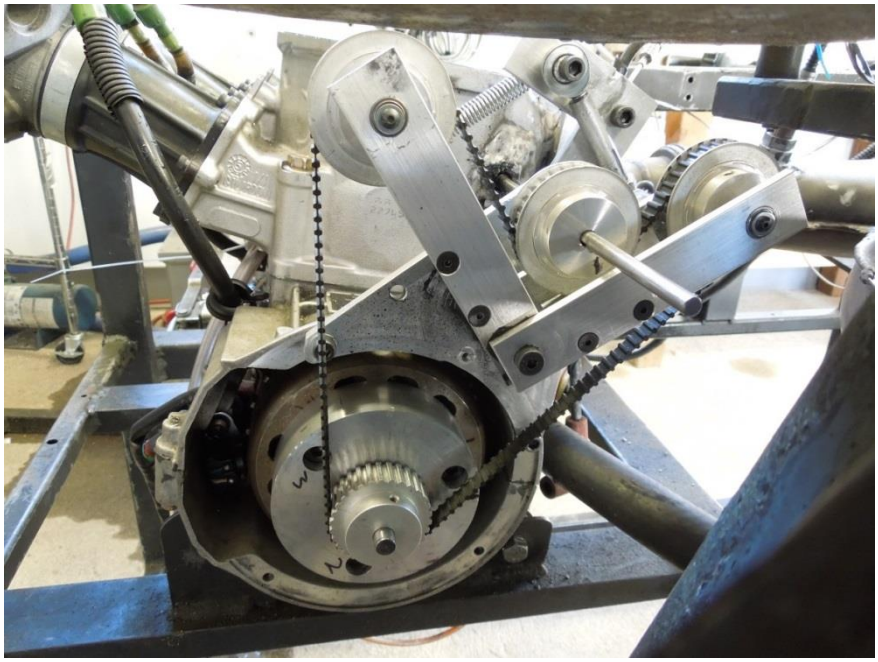

Figure 7: Belt Drive as Built

For the purpose of this research, the valve timing was manually adjusted at the crankshaft pulley by shifting the belt clockwise or counter-clockwise one or more cogged teeth. A yellow timing mark was painted on a tooth of the belt, that when lined up with the yellow mark on the crankshaft pulley, had the valve closing the exhaust port at 120° before top dead center (BTDC). This valve angle (VA) was defined as the base VA for the PR-SCT during all testing. Along with the painted yellow marks, a black line was placed on the crankshaft adapter and valve pulley. The black marks should align and point towards the shoulder bolt of the belt assembly arms when the valve timing is at the base angle. These verification marks were used to check the valve timing was correct and had not shifted. Once valve alignment was verified, the yellow mark on the belt could be shifted in the desired direction, to one of the other painted marks, or between two marks to achieve the desired valve timing.

Figure 8 shows the valve at its base position, with the timing marks aligned, and Figure 9 shows the marks for the different VAs on the crankshaft pulley.

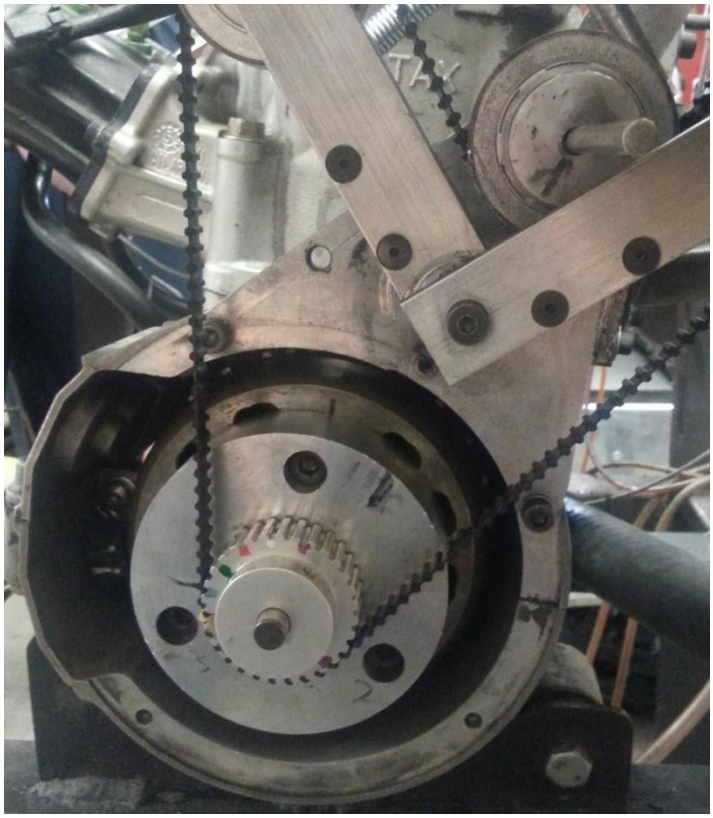

Figure 8: Valve Position at Base Angle

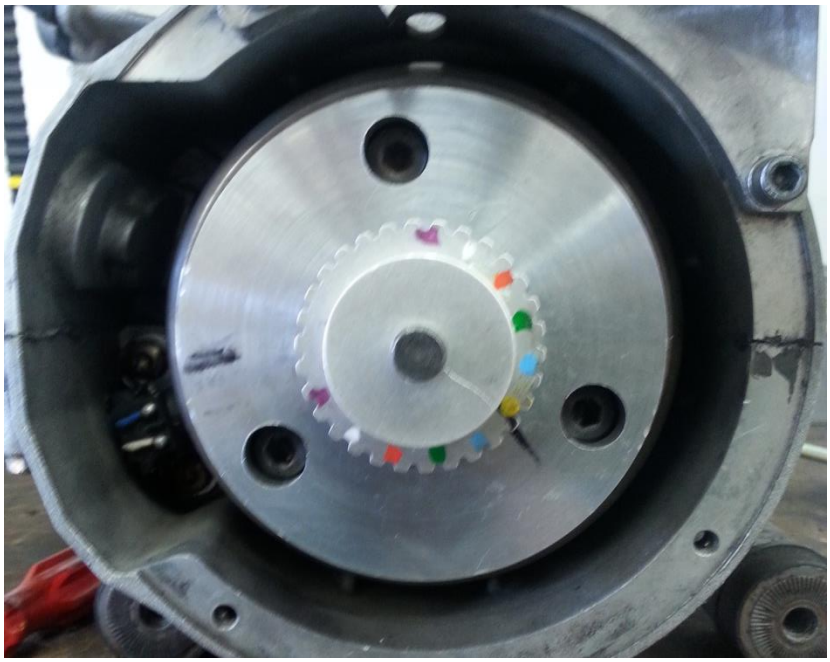

Figure 9: VA Positions

Each shift of cogged tooth represented a 5° change in valve timing, and each painted mark on the crankshaft pulley represented a 10° shift in valve timing. In Table 1, the valve timing for the corresponding colors and direction of rotation is shown.

Table 1: Valve timing

Mark Color	Belt rotated Clockwise	Belt rotated Counter-Clockwise
Blue	130° BTDC	110° BTDC
Green	140° BTDC	100° BTDC
Orange	150° BTDC	90° BTDC
White	160° BTDC	80° BTDC
Purple	170° BTDC	70° BTDC

3.1 Valve Face Remodel

3.1.1 Previous Test Results

Upon the completion of Hooper's testing, it was determined the PR-SCT valve did not have the desired effects on engine performance and exhaust emissions. [3] When comparing brake specific fuel consumption (BSFC), and exhaust emissions, the past PR-SCT used by Hooper performed better than Hooper's configuration 1 of the stock E-TEC engine, as expected.(Configuration 1 is a stock 600 Ski-doo E-TEC with its power valves in the up position). However, it was not able to match the results of the stock 600 E-TEC engine with its power valves in the down position, and typically positioned itself midway between configurations 1 and 2. It can also be seen that there is little difference between Hooper's configurations 4, 5, and 6, due to the limited change in valve position between configurations. Figure 10 shows Hooper's BSFC results at Hooper's operation point 1, 5200 RPM and 10% throttle. In Hooper's graphs the desired function is graphed versus injection angle (IA) and lambda. Injection angle is the crankshaft angle that fuel is injected at BTDC and lambda is the ratio of the stoichiometric air fuel ratio over the actual fuel ratio.

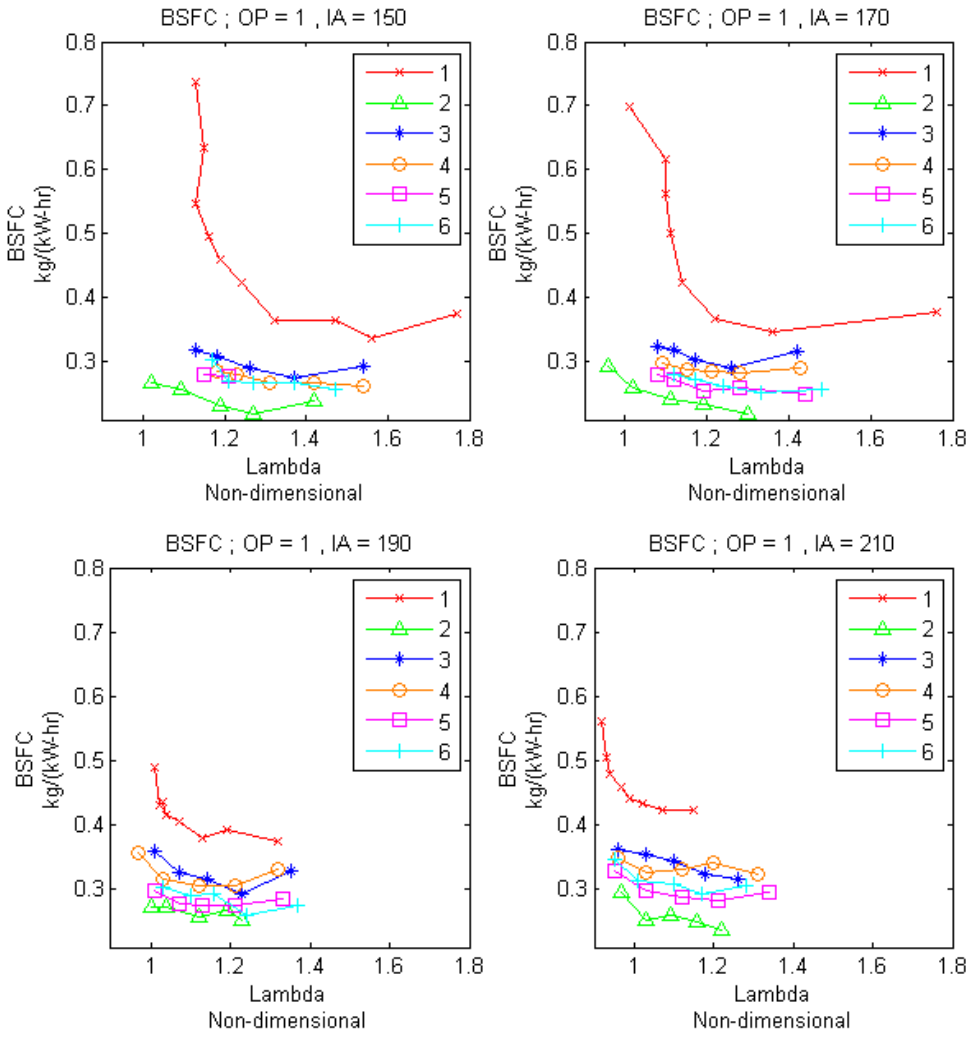

Figure 10: Hooper's Operation Point 1 BSFC results

An interesting result of Hooper's testing was, at 6000 RPM, the valve's effect on (BSFC) and exhaust emissions appeared to increase and cause a greater reduction over Hooper's configuration 1. [3] However, this effect was not able to be further studied by Hooper due to a failure of the valve shaft. Figures 11 and 12 show a total emissions comparison using an EPA five-mode emissions function at Hooper's operating point one and two. The total

emissions function gives points that would be deducted from the EPA emissions score. The EPA five-mode emissions test will be further explained in section 4.3.3.

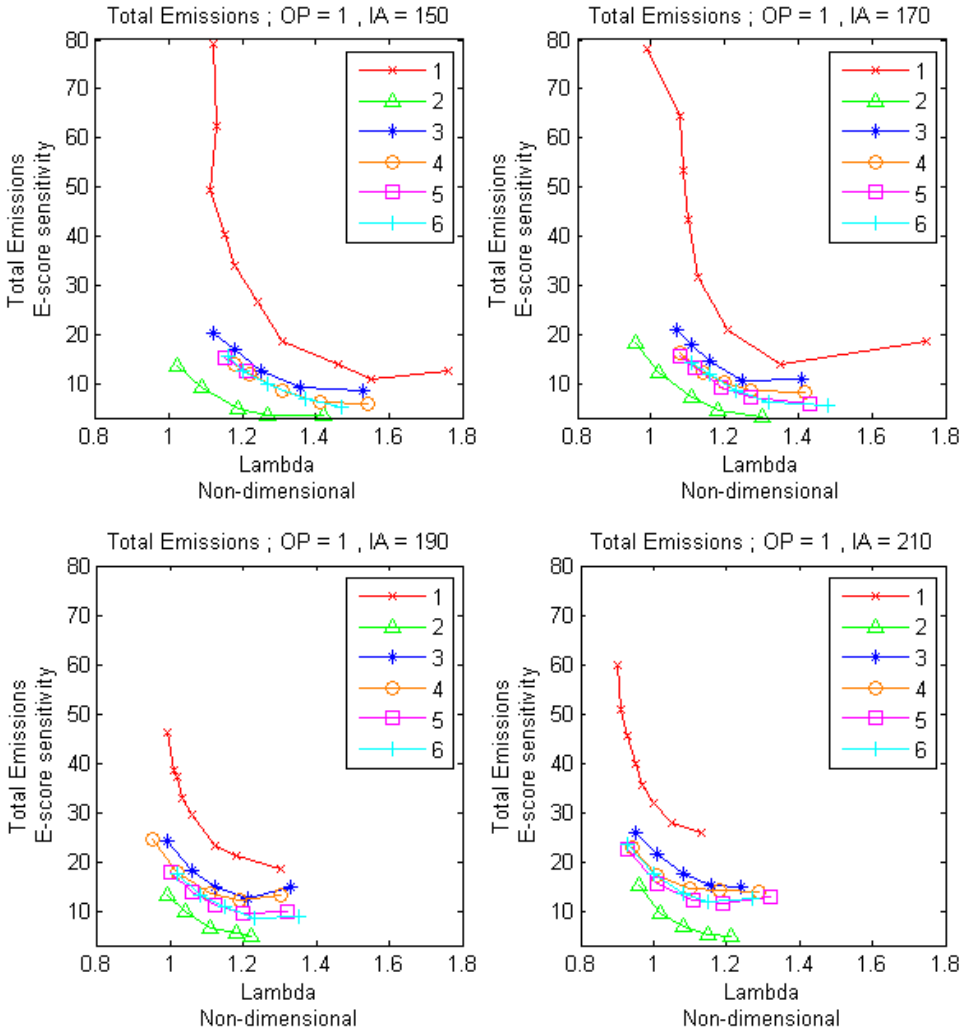

Figure 11: Hooper's Total Emissions at Operating Point 1

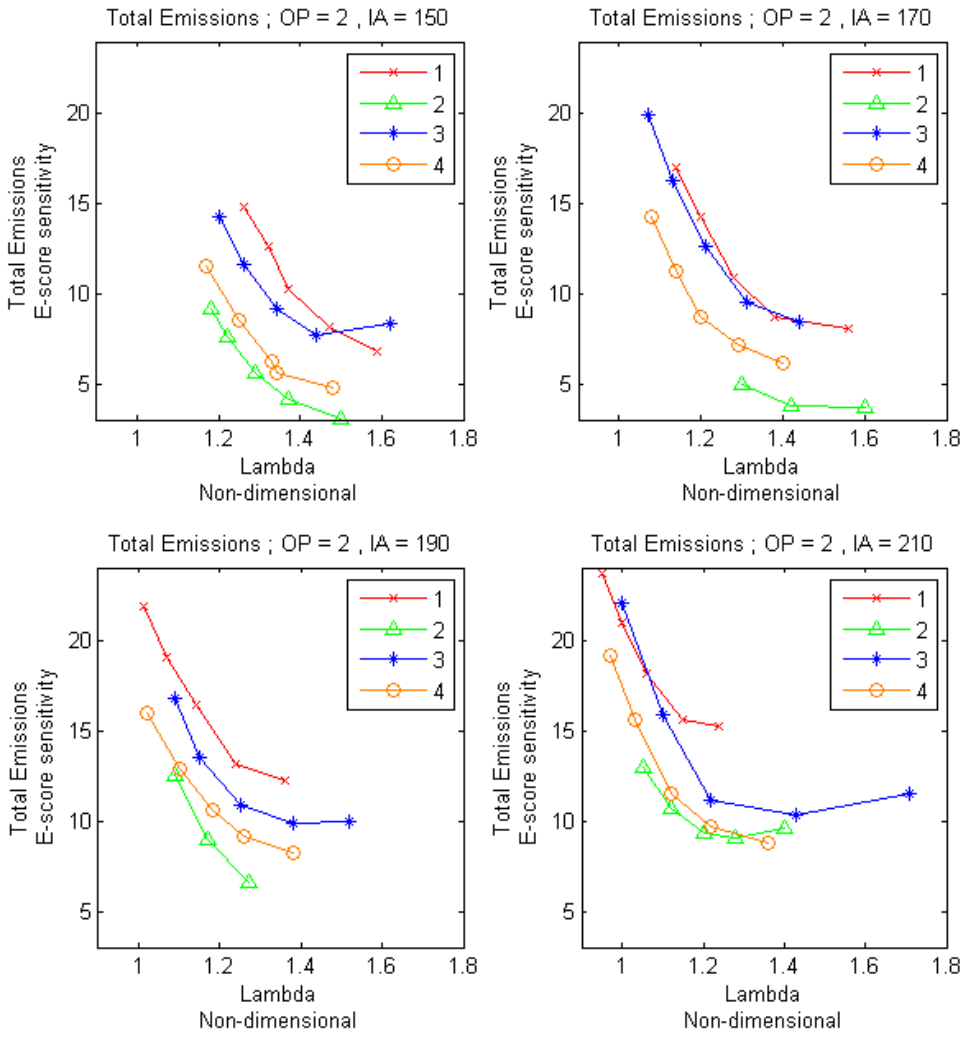

Figure 12: Hooper's Total Emissions at Operating Point 2

3.1.2 Valve Face Redesign

The likely cause of the initial valve's lack of trapping is spacing from the piston. The original design had the valve face spaced 0.120 inches from the piston. After speaking with individuals in the two-stroke engine industry, it was learned that for an exhaust valve, such as a power valve to be effective, it needed to be between 0.020 and 0.040 inches from the piston. [11] From these conversations and after reviewing Hooper's results, it was

determined a new valve within the recommended clearance was required. A simple redesign of the valve to have a tighter clearance to the piston was not an option. If the valve were to have a single hyperbolic face, like the original design, the outer edges of the valve would contact the cylinder and exhaust runner area. Machining clearances for this design were also not possible, as they would cause destruction of the exhaust runner and likely cause water leaks in the cylinder. The exhaust runner is the path in the cylinder from the exhaust port to the exhaust system. With this in mind, the valve face was redesigned to have a double hyperbolic face, as seen in Figure 13. This shape was chosen as it allowed the main face of the valve to be 0.040 inches from the piston, but also allowed the outer edges to be free of interference. This design also only required a small amount of hand grinding to the cylinder and exhaust runner to allow for proper clearance.

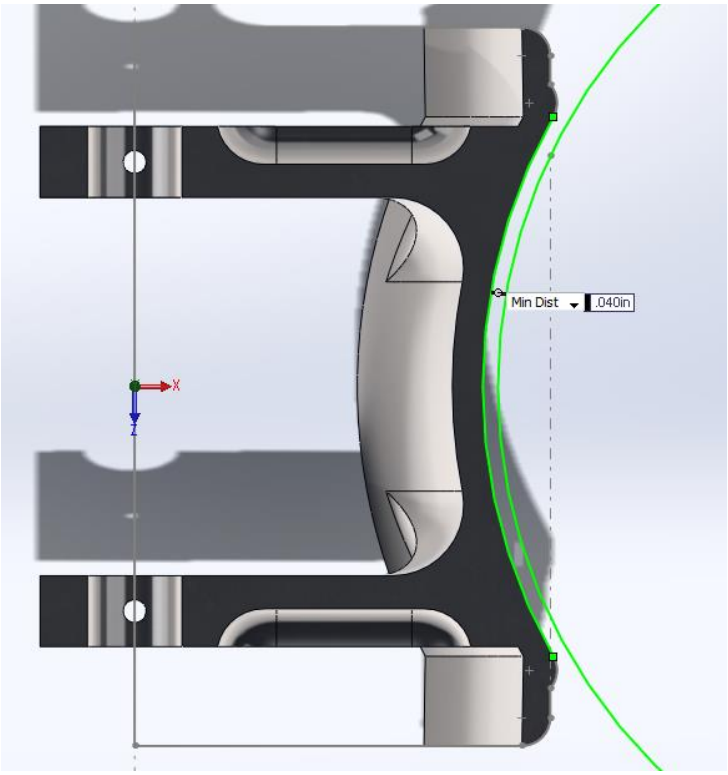

Figure 13: Sectioned view of valve to piston clearance

3.1.3 Valve Manufacturing

Prototypes of the valve design were printed using a rapid prototype Maker Bot 3-D printer. The printed valves allowed for clearance issues to be identified before manufacturing of the actual valves began, and also allowed for physical measurements to verify the 3-D model. Typically, the printed valves came out 0.010 inches undersized, but were still a useful step in manufacturing and implementation of the valve design, as they were able to be produced quickly and affordably. Figure 14 shows an example of a completed printed valve.

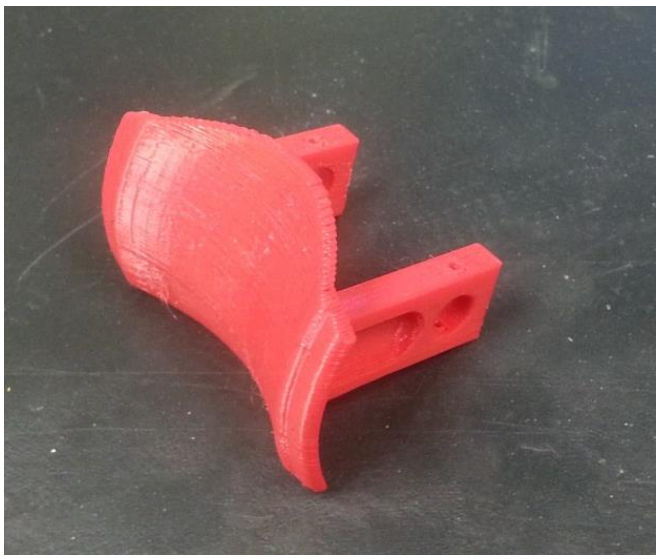

Figure 14: 3-D Printed Valve

The manufacturing process for the new valve design was very intensive, twenty hours of work on a Haas CNC mill was require for each valve. The use of previous valve CNC code and machining plans decreased the preparation time prior to manufacturing. A completed valve is shown in Figure 15.

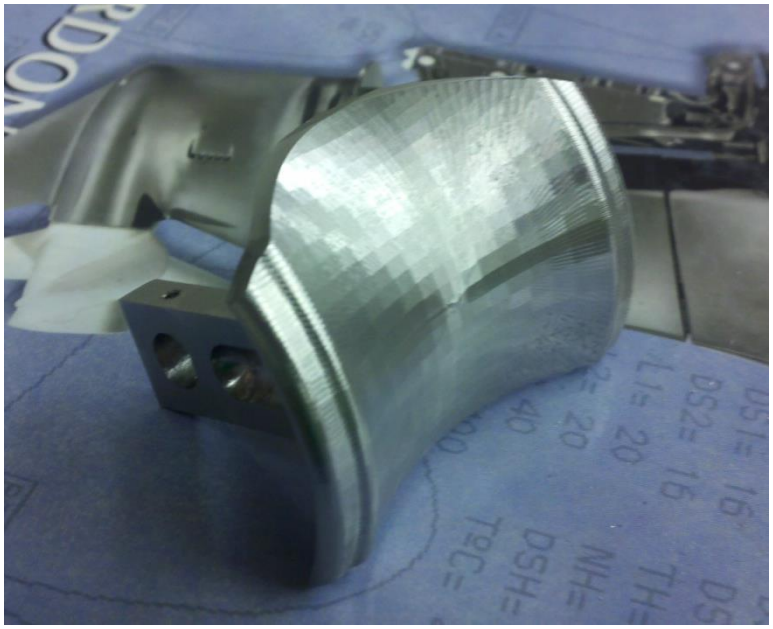

Figure 15: Completed Valve

4 Testing

4.0 Hardware Configurations

For this research, two engine configurations were tested. The PR-SCT engine without its valves in place, but with the valve shaft in place, and the PR-SCT fully assembled with a variety of VA. The PR-SCT will be compared to three engines from past research at UIdaho. Engine number is one is Hooper's configuration 4 at his test point one. The PR-SCT engine was fully assembled with the VA set to 120° BTDC, running at 5200 RPM and with a 10% throttle opening. The number two engine is the stock 600 E-TEC, calibrated by Hooper for his experiment. The final engine, number three is the factory calibrated stock 600 E-TEC engine. This engine was tested at UIdaho in 2010 to determine the emissions score and engine performance of the production 600 E-TEC. Additionally, the factory calibrated engine will have additional comparison data used from a published study done in 2009 at the Michigan Tech Keweenaw Research Center. [12]

4.0.1 Engine Control

The engines tested use E-TEC direct fuel injectors to control fuel injection quantity and timing. The injectors, along with all other engine functions, were controlled by an electronic control unit (ECU).

4.1 Testing Equipment

4.1.1 Dynamometer

The dynamometer used in this research is the University of Idaho's Borghi and Saveri 260-S eddy current dynamometer. The dynamometer is rated at 450 ft-lbs and 260 HP at 12000 RPM. The strain gage on the dynamometer has a nonlinearity of 0.05%, a non-repeatability of 0.02%, and a hysteresis of 0.03%. [13] The dynamometer is controlled by SuperFlow controls, which are capable of monitoring 34 channels of data, while managing engine RPM and power output. A steady-state test on the SuperFlow controller was used at each operating point to hold the engine at a specific speed and throttle point while collecting data from the system sensors at ten measurements per second. Data were also collected visually, to help determine the typical human error. For this research, an additional sensor in the form of an air flow rate turbine and intake plenum was added to the SuperFlow system. The turbine was used to record the flow rate into the engine for the calculation of scavenging ratio, volumetric efficiency, and other performance defining parameters. The plenum was designed for a volume three times larger than the individual cylinder volume of the 800cc Rotax engine that the UIdaho Clean Snowmobile Team uses for competition. The design of the plenum allows it to be adapted to any engine within the UIdaho capability. The plenum and air turbine are attached to the PR-SCT primary air box on the dynamometer, as shown in Figure 16.

Figure 16: Air Plenum and Dynamometer

4.1.2 Fuel

For this research, a Max machinery 710 fuel measurement system was used to supply fuel to the engine at the desired pressure, and to measure the flow rate of the fuel. The system is capable of taking the measurement of fuel consumption over a user defined period of time, which for this research was set at 30 seconds. The error in the measured fuel flow rate is 0.75% of the actual measurement. There is additional error in the fuel consumption measurement, as the timer is started and stopped by a user with a stop watch.

4.1.3 Emissions

Emissions were measured using a Horiba MEXA-584L portable five-gas emissions analyzer. The analyzer is capable of measuring CO, CO_2, NO_x, O_2 and HC emissions with relatively low error for an affordable and portable unit. During the 2013 CSC competition, the UIdaho's predicted E-Score using the Horiba analyzer only differed by 2 points or 1 percent from the actual measured value at competition using an EPA certified emissions bench. The error for the system is shown in Table 3 for all measured gases. Smaller error values, based on the unit measured, are also reported in the Horiba manual and can be used. In this research, the larger error values will be used, as the lesser values have restrictions on their usage. The error values used for the emissions analyzer and all other measurements are the percent error of the actual measurement, meaning for example a measurement of 3% CO by volume has an error of plus or minus 0.09% by volume according to Table 2.

Measured Gas	CO	HC	CO_2	O_2	NO
Unit	%Vol	PPM	%Vol	%Vol	PPM
Percent Error Measurement	3%	5%	5%	3%	4%

Table 2: Error in Horiba MEXA-584L Measurements

4.1.4 Air-Fuel Ratio

The air-fuel ratio of the engine was measured with an Innovate LM-2 wide band air-fuel ratio meter. During this research, air-fuel ratio was recorded as lambda, the actual air-fuel ratio over stoichiometric air-fuel ratio. The accuracy of the meter was found to be within 2%

of the value from the emissions analyzer by Dixon, while having a much faster response time. [4]

4.2 Testing Methods

During this research, two separate testing methods were used for data collection. The first method was used while replicating Hooper's experiment at Mode 4 of the EPA emissions test of a stock Ski-doo 600cc E-TEC engine. This is seen in Hooper's thesis as operating point 1 of configuration 4. In Hooper's experiment, the injection angle was set to a predetermined value, and the fuel quantity was swept at five evenly spaced points. The range of the fuel quantity sweep was determined by finding the lean and rich limit of the injection angle. The lean limit was determined by reducing the fuel quantity till a 10% drop in torque was seen, and the rich limit was determined by increasing the fuel quantity until the CO percentage reached 3%. This method was replicated at three other injection angles, and from these data, an optimum point can be found. The second testing method, used for the five-mode emissions test, was a 3-D calibration method. The UIdaho CSC team uses this method during calibration of its competition snowmobile. The method starts by sweeping VA positions, while holding a constant injection angle and constant lambda value. After the VA is swept, the optimum angle is determined by analyzing run quality, power output, BSFC, and exhaust emissions. The injection angle is then swept at the optimum value angle and the same constant lambda value from earlier. The optimum injection angle is then determined and fuel injection quantity is then swept. The range of the sweeps varies depending on the load and RPM of the engine, with the only requirement that a clear optimized point of the desired function is determined. A way to clearly determine the optimized point is to create a J-hook. An example of a J-hook is shown in Figure 17, where

VA was swept until a clear minimum was determined for the emissions score sensitivity and a local maximum was found in each direction of the minimum value.

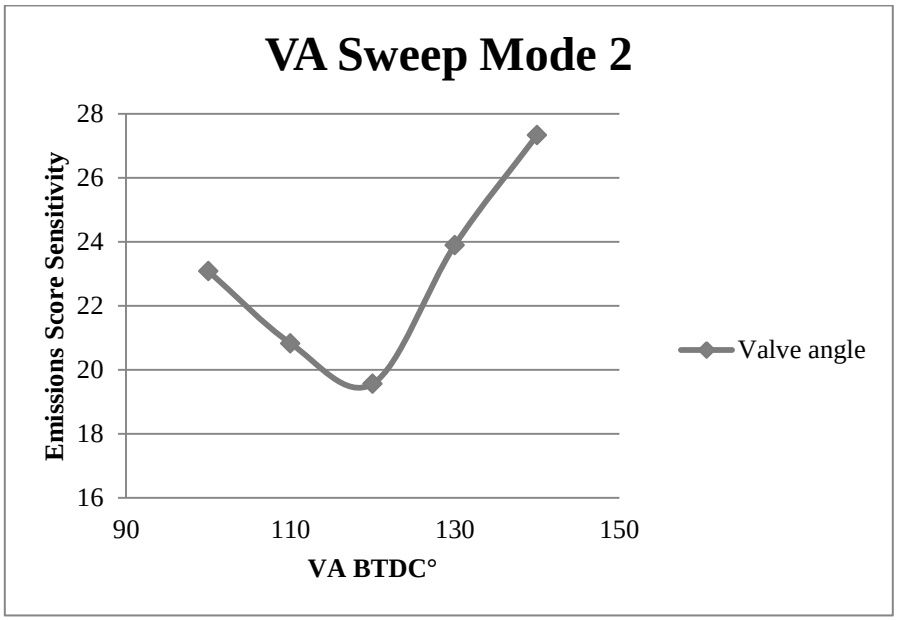

Figure 17: Optimization of VA and Emissions Score

Another method of 3-D calibration, considered for this experiment involves holding exhaust %CO constant instead of lambda and is referred to as emissions tuning. Holding %CO provides a higher accuracy in clearly determining an optimized point, as the error and repeatability in measurement of %CO is much better the measurement of lambda. While emissions tuning provides a higher accuracy result, it was not chosen for this experiment, as it is time intensive. The response time of the emissions analyzer is much slower and typically requires one minute of stabilization at a point to determine the %CO value, while response time of the lambda meter is almost instantaneous. Comparing the two methods, Welch found that holding lambda constant was within 6% of the true optimized point found

by holding %CO constant. It was recommended by Welch that lambda be held constant when determining rough calibration of an engine to reduce calibration time. [14]

4.3 Test Plan

4.3.1 PR-SCT Without Valves

Before testing the PR-SCT with the redesigned valves, testing of the engine without the valves was necessary to determine peak speed and load engine characteristics and limitations caused by modification to the stock exhaust runners. The valve shaft was placed in the exhaust runners to help prevent exhaust leaks, but the belt was not installed. With the engine at full load engine, engine speed was slowly increased until the high limit was reached. The limit was determined by a significant decrease in measured torque and/or run quality.

4.3.2 Replicating Hooper's Experiment

To compare the effectiveness of the redesigned valve face, part of Hooper's experiment was replicated. The configuration and test points chosen were configuration four and test points one and three. Configuration four was chosen, as it was the only configuration of Hooper, where the valve position was accurately known and had the least tendency for the belt to slip. Test point one was chosen as it has a lower power output, putting less stress on components, as well as being EPA mode 4 for a stock 600cc E-TEC engine. Test point three was also chosen, as it allowed for a wide open throttle (WOT) performance comparison of the original PR-SCT valve to the remodeled valve face, as the original valve was never tested at maximum RPM and torque.

4.3.3 EPA Emission Modes

The EPA five-mode emissions test, used for testing of all production snowmobiles, was created in 1998 by the Southwest Research Institute (SwRI). The test was created for the International Snowmobile Manufacturers Association (ISMA), due to interest in snowmobile emissions. [15] The test is designed to replicate real world use of a snowmobile engine, with higher weighting at the points of highest use. The test begins with a slow power sweep at wide open throttle (WOT) to determine maximum power and the engine speed at which it occurs. Table 4 shows the different mode points and their corresponding speed, torque and weighting value.

Mode Point	1	2	3	4	5
Speed (% of Rated)	100	85	75	65	Idle
Torque (% of Rated)	100	51	33	19	NA
Weighting Factor (%)	12	27	25	31	5

Table 3: The Five Modes Used for the EPA Emissions Test

Once maximum power is found, the torque value at maximum power is defined as 100% torque. After mode one is determined, the mode points are then tested in order from one to five, and the results are compiled for the final emissions score or "E-Score" based on Equation 9. The EPA requires a minimum score of 100 for a snowmobile, while also imposing limits on brake specific HC and CO. Stricter limits of an E-Score of 170, and lower limits on brake specific HC and CO emissions are required by the National Park

Service (NPS) for a snowmobile that is allowed in sensitive areas such Yellowstone National Park.

$$E\text{-}Score = \left[1 - \frac{HC + NO_x - 15}{150}\right] * 100 + \left[1 - \frac{CO}{400}\right] * 100$$

Equation 9: EPA Emissions Score

Due to extremely rough base calibration of the engine, the actual mode points were not determined. Instead, the approximate mode points were found by varying throttle position until the percent torque for the actual mode point was reached. Upon determining throttle position, it was held constant during the 3-D calibration method. Once a complete calibration of the engine is done, the actual mode points could be found. This, however, is beyond the scope of this research. For this research, the order the mode points were tested was changed in attempt to gain as much possible data, before failure of a component ended testing prematurely. Power sweeps at mode 1 were first completed to find maximum power and RPM, then calibration of the modes was started at mode 5 working towards mode 1.

4.4 Error in Propagation in Measurement

When looking at the error of measurements, the errors of each of the individual pieces of equipment used are combined using the root sum squared method for a total measurement error. An example of this would be the BSFC measurement as shown in Equation 10 with a total error of 0.75%. Table 5 shows combined error for measurements.

$$BSFC_{error}\% = \sqrt{{Fuel_{error}}^2 + {Power_{error}}^2}$$

Equation 10: Root Sum Squared Method for BSFC Error

	BSFC	CO	HC	CO_2	NO	TE	E-Score	BMEP
Measurement Error of Reading	0.75%	3.9%	5.05%	5%	4.07%	7.68%	7.22%	0.05%

Table 4: Error in measurements

5 Replication of Hooper's Experiment Results

Emissions data in this chapter will be reported in both brake specific (g/kW-hr) and fuel specific (g/kg fuel) units, as Hooper presented his data as brake specific emissions, and published data on the Ski-doo 600 E-TEC is published in fuel specific emissions. Power output data will be presented as brake mean effective pressure (BMEP), as it provides a measure of power that allows comparisons to engines of different power levels and displacements. Corrections have been made to Hooper's data, as his torque values were incorrect. A torque placed on the dynamometer head by its cooling pump, caused a 3 ft-lb increase in measured torque values. [3] Corrections were also made to Hooper's mass based emissions, as an error was found in Hooper's spreadsheet in the conversion of volumetric based emissions to mass based. All percentage differences reported take into account the error of the measurement. The error was assumed to have a negative effect on the PR-SCT engine, and a positive effect on the other engines. For example when looking at BSFC the PR-SCT was assumed to be 0.75% larger while the comparison engine value was assumed to be 0.75% lower.

5.0 Fuel Efficiency

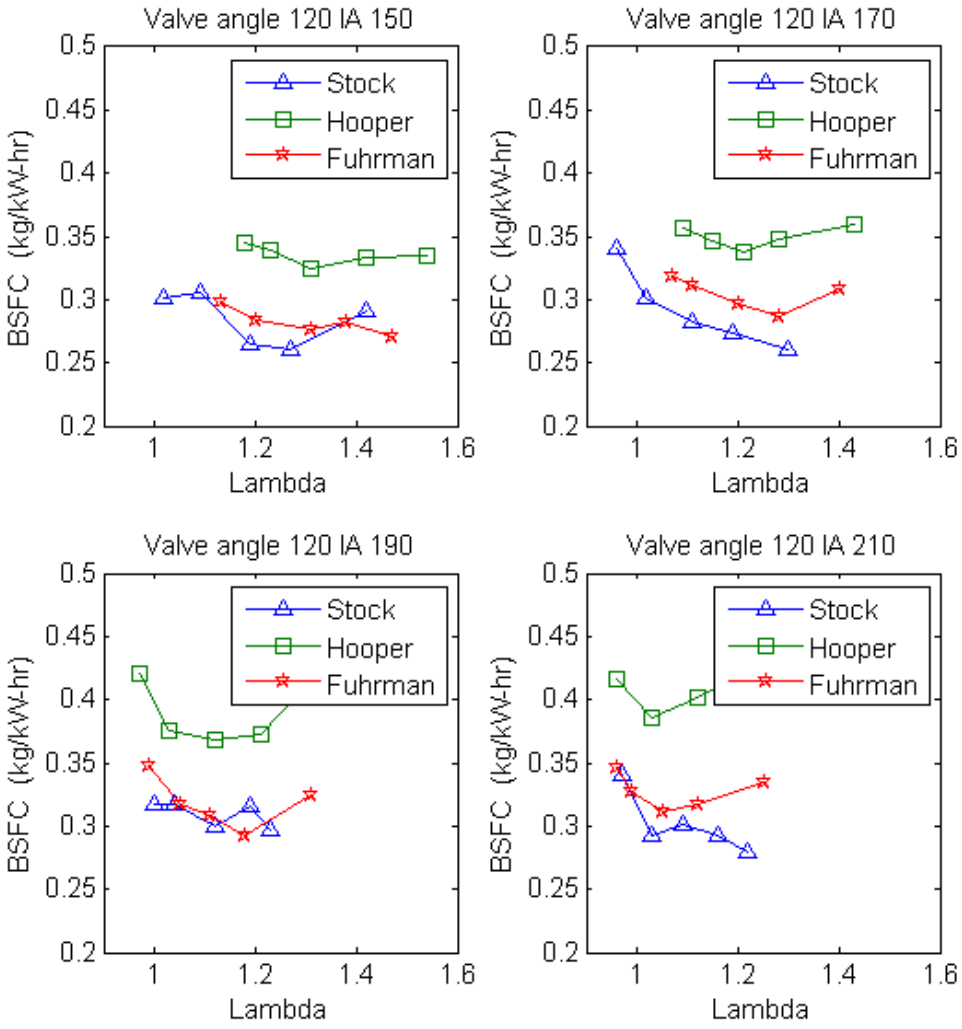

Figure 18: BSFC Data from Replication of Hooper's Experiment

The comparison of the engine's BSFC is shown in Figure 18. When analyzing BSFC, a large decrease is seen compared to Hooper's results across the entire spectrum of data, with the PR-SCT surpassing the stock engine at some test points. Comparing the optimum BSFC points of the three engines, a 20.3% reduction in BSFC was seen between Hooper's configuration and the current PR-SCT configuration. The PR-SCT was not able to surpass

the stock configuration at its optimum point, with a 3.8% difference between the stock engine and PR-SCT.

5.1 Emissions

5.1.1 HC

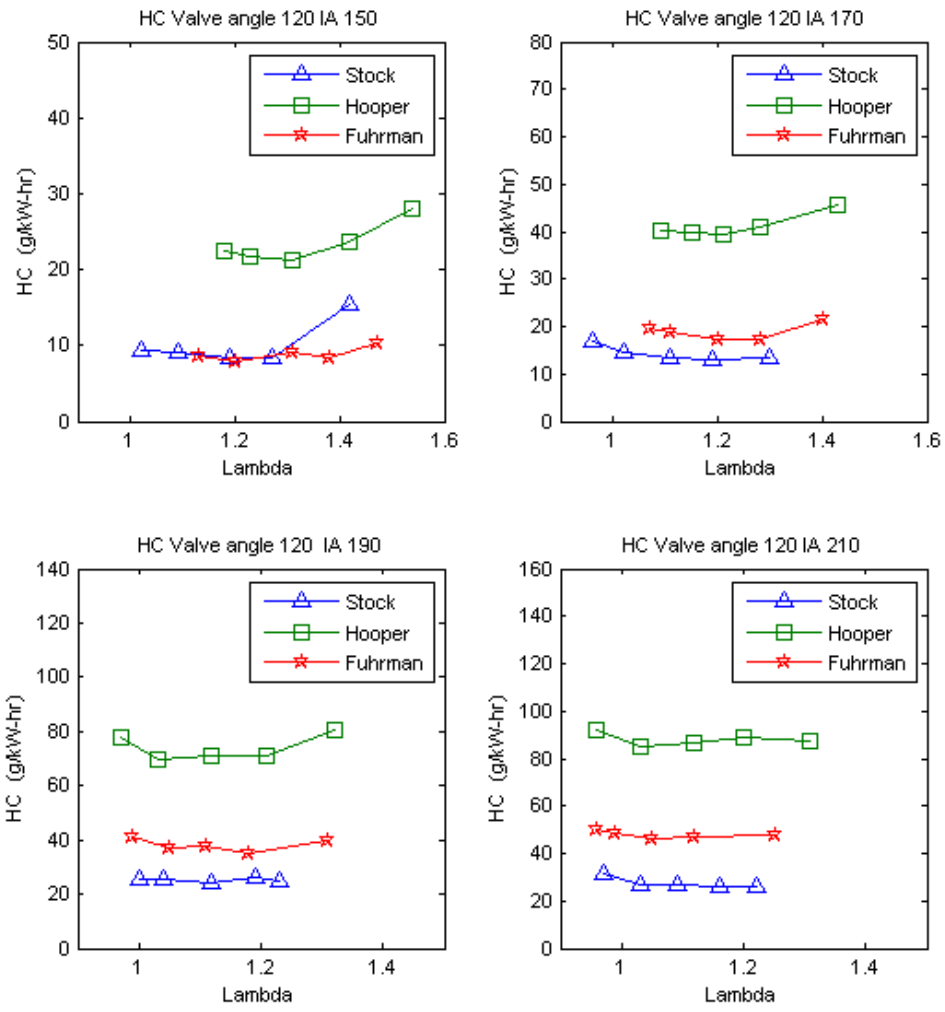

Figure 19: HC Comparison Data

The trend of the performance of the current PR-SCT configuration greatly surpassing that of the first iteration of the PR-SCT continues when comparing HC emissions. Comparing optimum points of the current PR-SCT configuration to Hooper's, Hooper's configuration has 155% more brake specific HC emissions. The large reduction in HC emissions was expected since the new valve design has a much tighter tolerance to the exhaust port, and provides a much higher theoretical TE. The PR-SCT was also able to match Hooper's calibration of the stock engine within the error of measurement comparing optimum results. Comparing the PR-SCT with published emissions results from a factory Ski-doo E-TEC at mode 4, the PR-SCT has a 1% reduction in HC emissions. Then comparing the PR-SCT with UIdaho CSC testing of a stock 600 E-TEC engine a 6% percent reduction in HC is seen.

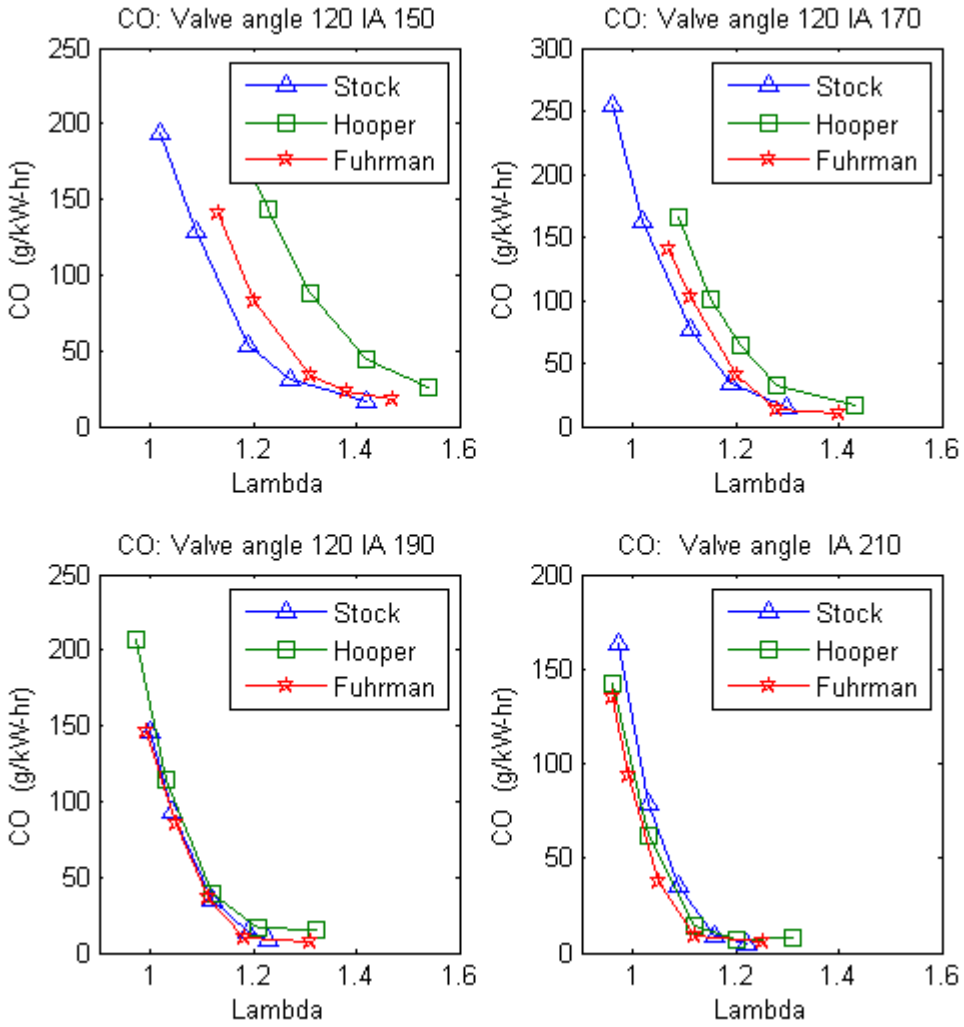

Figure 20: CO emissions comparison

A comparison of CO emissions from the replication of Hooper's experiment means little, as CO emissions were used to define the fuel injection quantities effectively, making all of the CO values the same. CO emissions are an indication of combustion performance and, as discussed earlier, can be used instead of lambda when performing calibration sweeps. In defining the lean limit, Hooper used a 10% reduction in measured torque. In practice, this point was crudely measured making no two lean limits comparable.

5.1.2 Total Emissions

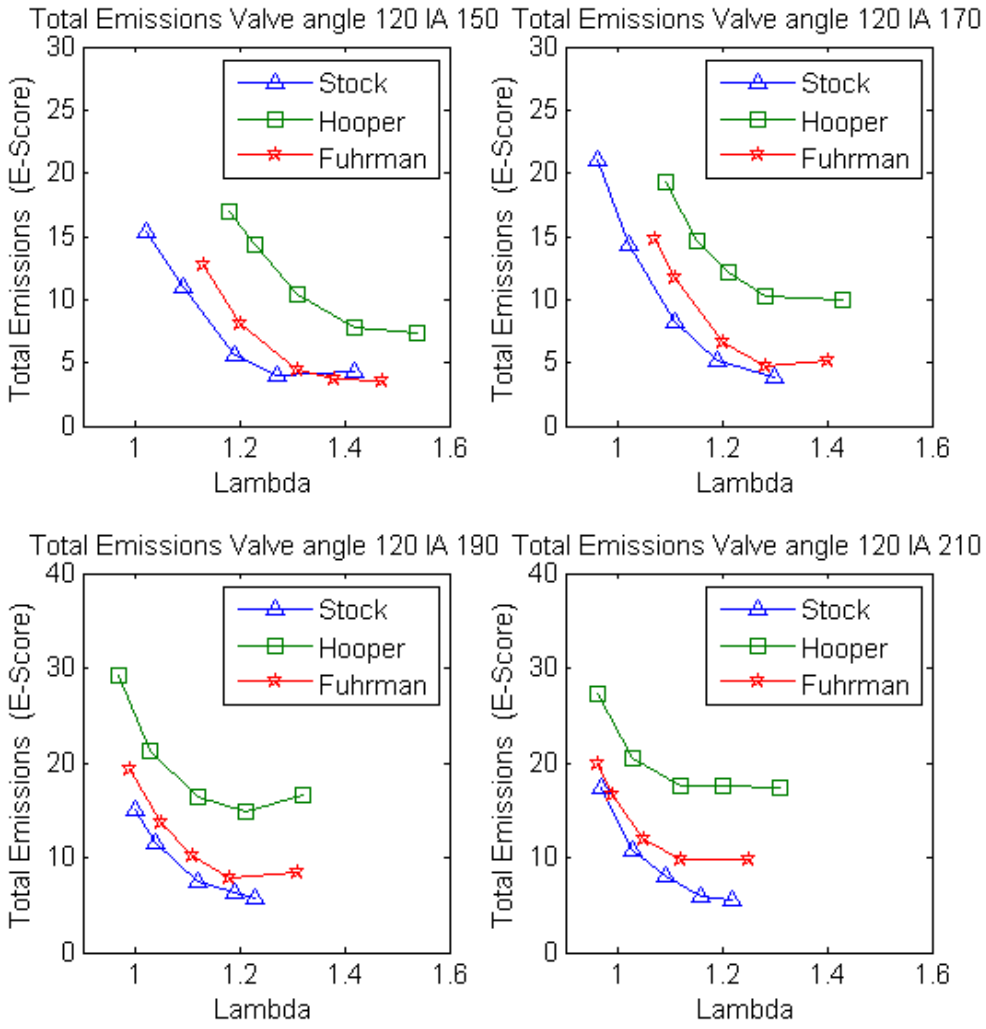

Figure 21: Total Emissions Comparison

The total emissions is based on the EPA emissions score and is a measure of how many points are subtracted from the perfect E-score of 210. Total emissions follow the trend of HC emissions of the current PR-SCT, providing a large reduction compared to Hooper's, and a small reduction, when compared to the Hooper's calibration of the stock engine. Comparing optimum total emissions points, the current PR-SCT provided a 98.6% reduction

compared to Hooper, and was able to match Hooper's calibration of the stock engine within the error of the measurement. Measurements errors were again assumed to favor the comparison engines and not the current PR-SCT engine.

5.2 Power output

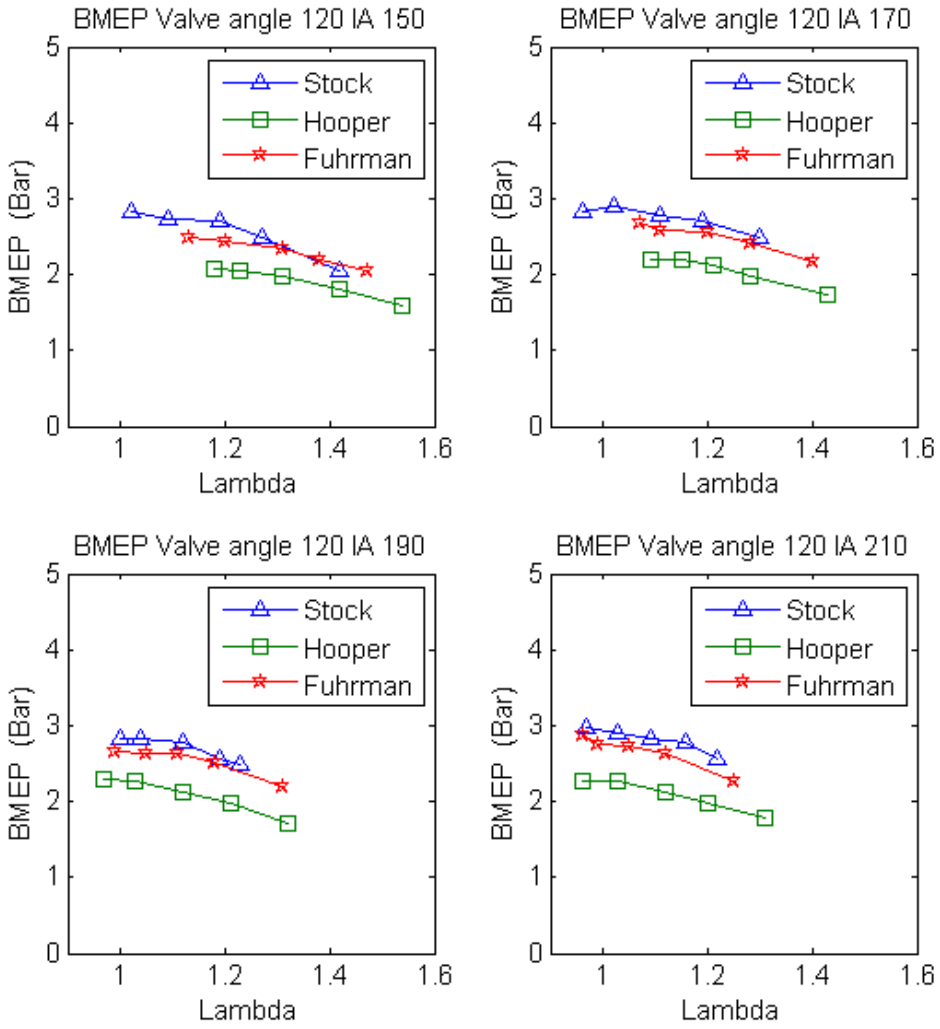

Figure 22: BMEP Comparison

BMEP results follow the same trend as other reported results above, with the current PR-SCT a large improvement over Hooper and close to stock engine. The current PR-SCT

provided a 24.3% increase in BMEP over Hooper, when comparing optimum points. Comparing the current PR-SCT to Hooper's calibration of the stock engine, the PR-SCT produces 4.1% less BMEP. While it is disappointing to not match the BMEP of the stock engine, the PR-SCT is now competitive with it.

5.3 Other observations

5.3.1 Wide Open Throttle Comparison

An additional test point of Hooper's was WOT at test point one. Hooper's calibration of the stock engine can only be compared with BMEP at this point, as fuel measurements are missing. Comparing BMEP, the difference between the current PR-SCT and the stock engine, the PR-SCT produces 11.2% less BMEP compared to the stock engine. Surprisingly, the difference between Hooper and the current PR-SCT decreased at this test point to 13.9%. When analyzing HC emissions, the current PR-SCT achieved a major reduction over Hooper's with a 262% decrease in brake specific HC emissions. The current PR-SCT does this with a 39% decrease in BSFC compared to Hooper's PR-SCT.

5.3.2 Trapping Efficiency

Trapping efficiencies reported in this section are fuel trapping efficiency and not air trapping efficiency, as conditions are not met for air trapping efficiency to be accurate. The trapping efficiencies for the three engines at Hooper's test point one and WOT are shown in Table 5. At both test points, the current PR-SCT appears able to match the stock engine and surpass Hooper, though this cannot be verified, as the trapping efficiency measurement error is greater than the differences in the engines

.

Operating Point	Stock Engine	Hooper PR-SCT	Fuhrman PR-SCT
Hooper Test Point 1	97.6%	93.5%	97%
WOT	63%	61%	70%

Table 5: Fuel Trapping Efficiencies at Hooper's Test Point 1 and WOT at 5200 RPM

6 EPA Emissions Results

6.0 Determining Mode Points

Power sweeps were performed, as specified by the EPA test guidelines, of a full throttle slow RPM sweep, to determine peak torque and RPM at peak torque. When the engine was run without the valves, the maximum engine speed for the engine was 7000 RPM. Attempting to go beyond this point resulted in misfire in cylinder one, likely due to excessive EG, making the charge in the cylinder incombustible. After installation of the valves, the maximum RPM was determined to 6900 RPM, though maximum torque occurred at lower speed of 6300 RPM. A VA of 90° BTDC was initially tested, as it was thought to provide the best balance between negative effects on pipe performance and exhaust flow restriction during scavenging. Figure 23 shows the SAE corrected HP and torque values from the power sweeps. A VA of 85° was chosen, as it provided the second best torque value, while having the best run quality, along with being capable of reaching the maximum engine speed. Emissions and BSFC were not considered when determining the ideal VA at mode one, as run quality and maximum power were viewed as more critical. Maximum torque occurred at 6300 RPM, making 48.1 ft-lbs and 57.7 HP.

Mode Point	1	2	3	4	5
Speed RPM	6300	5350	4700	4050	Idle
Torque ft-lbs (% of Rated)	48.1	24.5	15.8	9.1	NA
Weighting Factor (%)	12	27	25	31	5

Table 6: Actual Mode Point RPM and Torque Values

Table 6 shows the target RPM and torque values for each mode point based upon the maximum torque and RPM of the PR-SCT. An important note, the mode points are not correct for the EPA 5-mode test, as they were based on maximum torque, instead of the measured torque at maximum power. This mistake was due to the author incorrectly interpreting the definition of maximum torque used in test

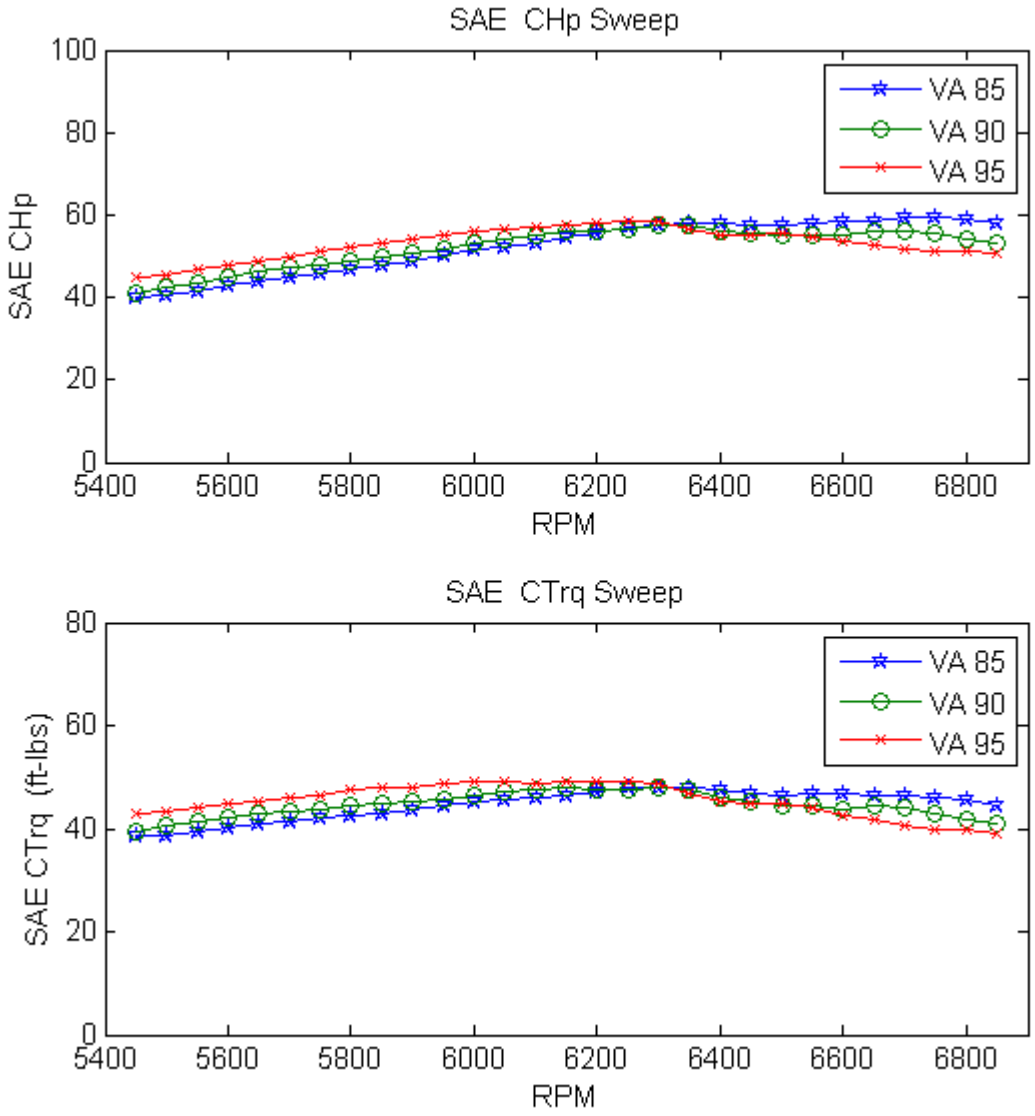

Figure 23: Mode 1 Power Sweeps

6.1 Brake Specific Fuel Consumption and Trapping Efficiency

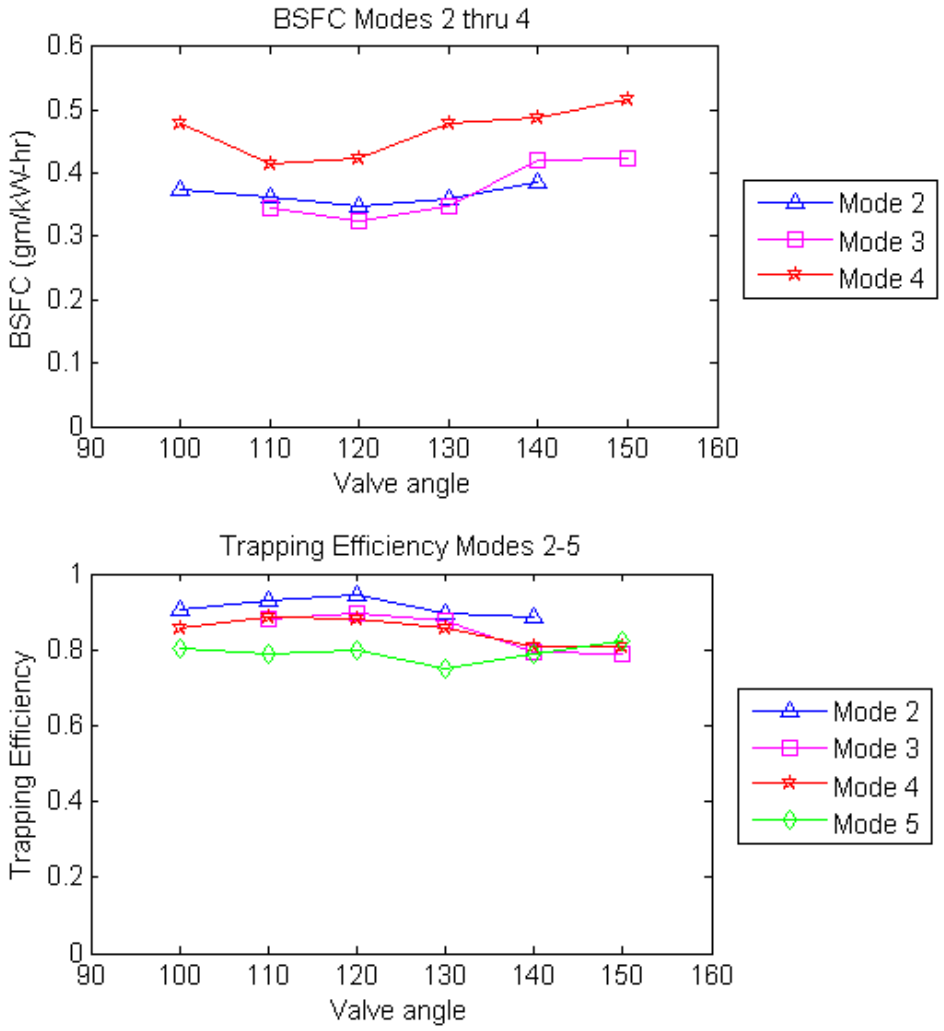

Figure 24: BSFC and TE Modes 2 thru 5

When analyzing the effect of VA on BSFC, it appears a VA of approximately 120° BTDC provides the optimum point for modes 2 and 3, where 120° BTDC is the point at which the transfer ports are closed. However for mode 4, a later VA provides a more optimum point,

with a 1.85% reduction in BSFC. This difference is within the error of the measurement. The later VA still may be correct, as the calibration of the engine around mode 4 is extremely rough. The engine struggles between making enough power at this point, and making roughly double the desired torque value. More time spent mapping the engine around this point should be able alleviate this problem and could provide clearer results.

Looking at TE, mode 4 appears to continue the trend of having an optimum at a later VA, but with very little difference between a VA of 110° BTDC and 120° BTDC. The important mode to notice, when looking at TE, is mode 5. An extremely early VA provides the highest TE, which was expected, as the trapped compression ratio is increased with the earlier VA. What was not expected, however, was at the VA between the optimum point and the base VA a higher BSFC than at the base VA was found. During the VA sweep at mode 5, engine parameters were not manually changed. An idle controller was used to keep a steady engine speed, as no load was applied by the dynamometer. The idle controller varies fuel quantity as needed to maintain the desired idle. During testing of the base VA, the idle controller moved to a leaner lambda value, which may explain the high TE of the base VA. Neither value, however, can statistically be proven better or worse, as the difference between the two measurements is approximately 2% and the error in TE measurement is 7.6%

6.2 Hydrocarbon Emissions

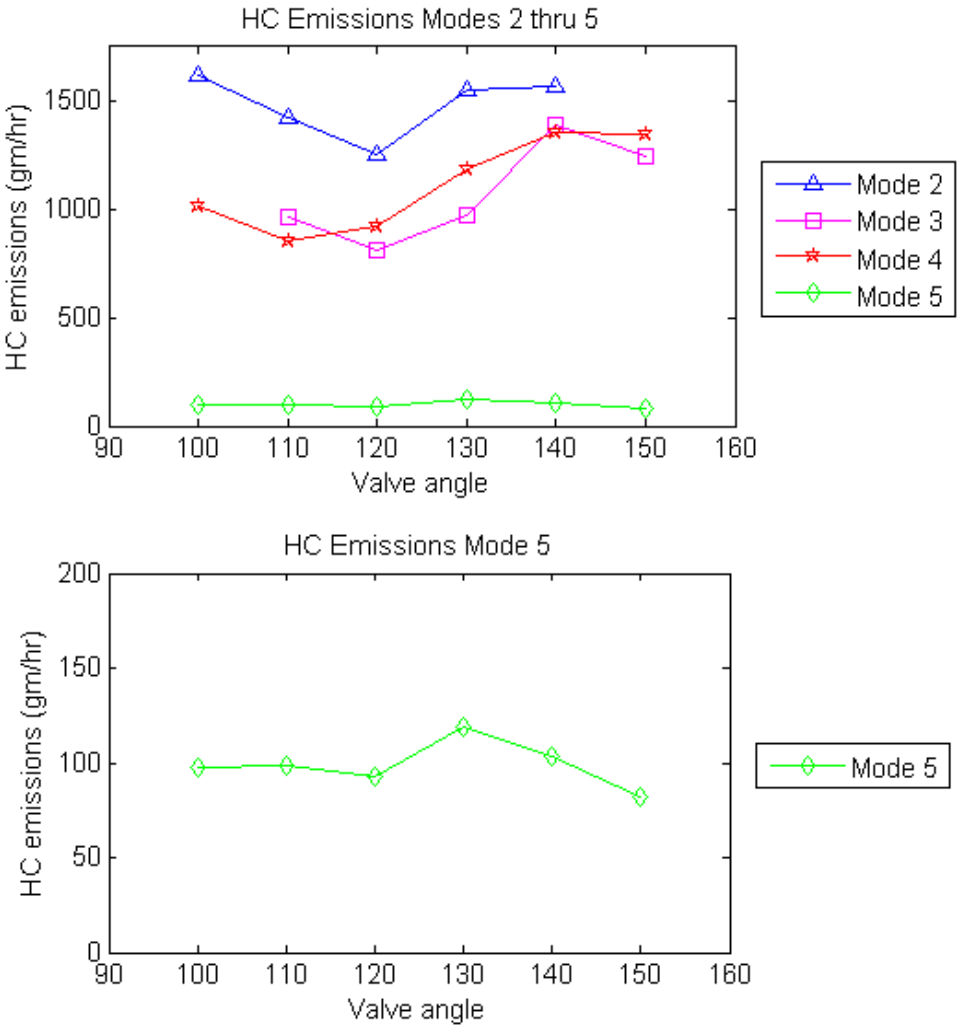

Figure 25: HC Emissions Modes 2 thru 5

Analyzing HC emissions shown in Figure 25, the optimum VA for modes 2 and 3 can be determined at 120° BTDC. The optimum VA angle for mode 4 appears to follow the trend being at 110° BTDC, this cannot be verified though as the two positions are statistically identical. Looking at mode 5 the optimum VA can be determined at 150° BTDC taking into account the error in measurement of HC emissions

6.3 Carbon monoxide Emissions

Looking at the CO emissions shown in Figure 26, the trend of the optimum point of mode 4 being at a later VA than modes 2 and 3 becomes inverted. Modes 2 and 3 optimum VA for minimum CO appears to be 110° BTDC and mode 4's optimum VA appears to be 120° BTDC. Mode 3 is shown on the smaller scale bottom graph of Figure 26, as it was tested at a leaner lambda value during its valve sweep. These leaner values caused problems when analyzing the CO emissions, as the emitted values are within the error of the analyzer. The large spike in CO emissions at mode 3 and VA of 140° is important to note. During testing of PR-SCT, an oscillation in engine performance was found. The oscillation would typically cause a temporary increase in CO emissions of over 100%, along with a decrease in the measured lambda value. The oscillation also caused small increases in power output, along with an audible exhaust tone change. HC and all other emissions were only minimally affected by the oscillation, with increases within the measurement error.

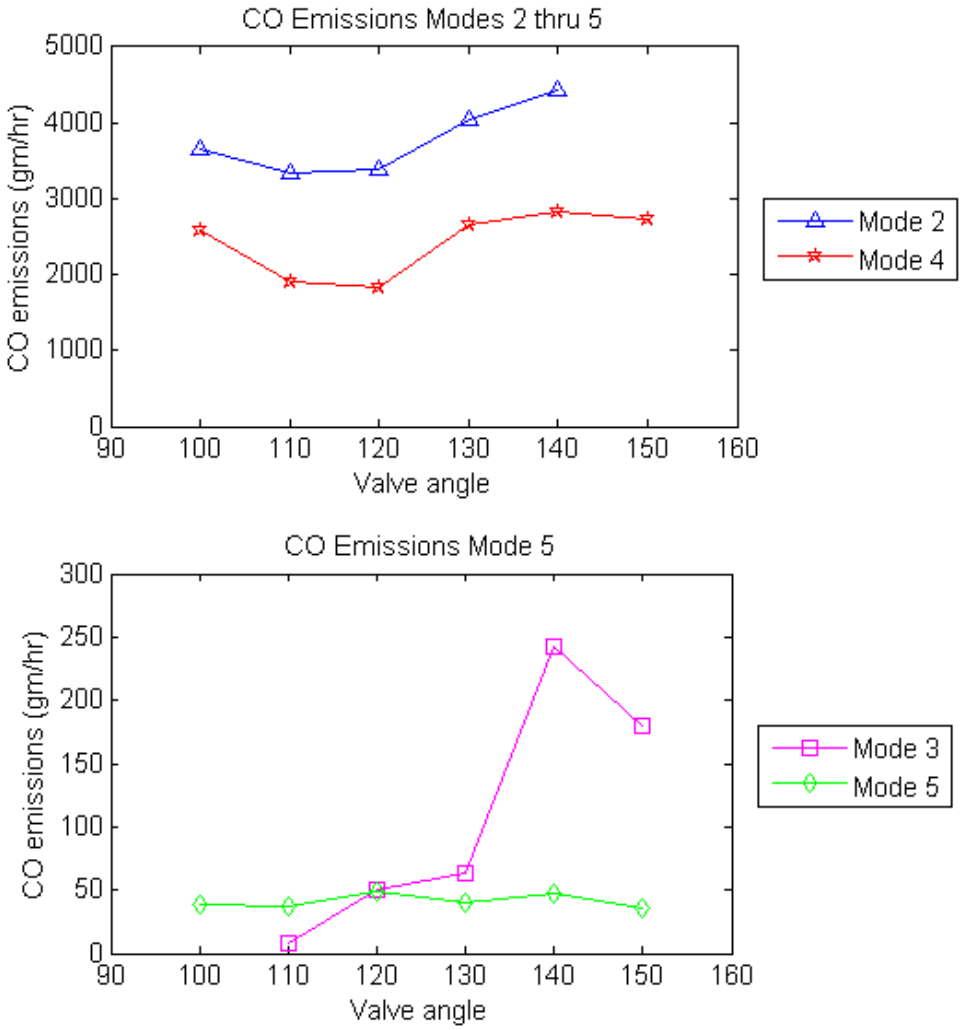

Figure 26: CO Emissions Modes 2 thru 5

6.4 Total Emissions and Brake Mean Effective Pressure

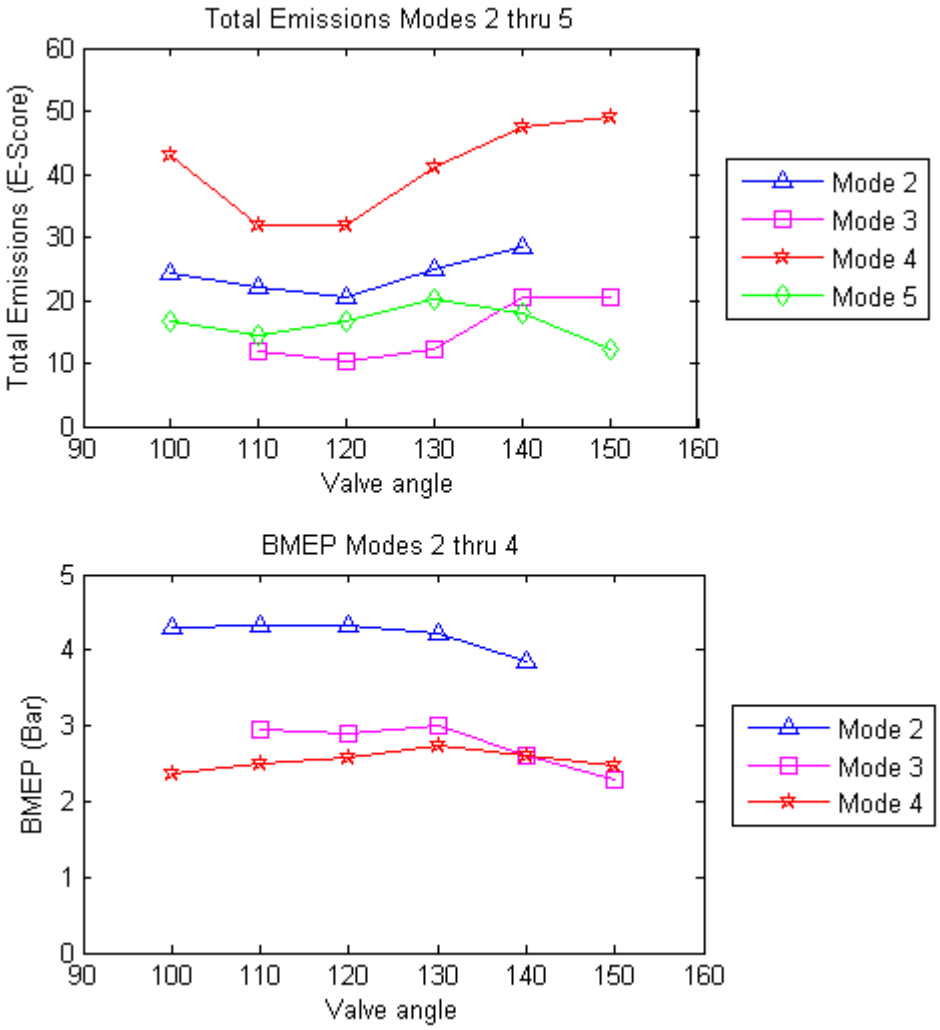

Figure 27: Total Emissions and BMEP Modes 2 thru 5

When analyzing total emissions shown in Figure 27, the optimum VA for modes 2 and 4 is likely between 110° and 120° BTDC, when accounting for measurement error. This follows the trend presented by all other measured results. An optimum VA for mode 3 appears discernible with a VA of 120° BTDC being 6.2% better than a VA of 110° BTDC. This

however is not able to be defined as the CO emissions used in this calculation, are within the error of the CO measurement. When accounting for this, the optimum VA for mode 3 is likely between 110° and 120° BTDC. The optimum VA for mode 5 however is discernible when looking at total emissions. The VA of 150° BTDC provides the optimum point, and is 11% better than a VA of 120° BTDC.

6.5 EPA E-Score Comparison

The most important comparison for the performance of the PR-SCT is against that of the engine on which it is based upon- the Ski-doo 600cc E-TEC. In this portion of the research, the PR-SCT is compared to data taken by UIdaho CSC team on a stock engine, along with being compared to published data on the stock engine. Values for published stock engine were taken with higher accuracy equipment, but required interpolation of the graphs to determine the values presented.

Looking at CO emissions in Figure 28 and HC emissions in Figure 29, the most notable thing is the inverse emissions characteristics of the PR-SCT. CO emissions are much lower at each mode point than for the stock engine, with the PR-SCT well within the NPS CO limit of 120 g/kW-hr, creating only 66 g/kW-hr. Analyzing HC emissions, the PR-SCT has much higher levels than the stock engine at each mode, with PR-SCT meeting only the EPA on HC + NOx limit of 90 g/kW-hr, producing 65 g/kW-hr. An additional measurement to note in this comparison is the oxygen content of the exhaust. The oxygen content of the PR-SCT engine is at minimum 30% higher than the stock engine. Looking at these three emission gases together and the inversion of the emissions characteristics compared to the stock engine, it appears the combustion flame on the PR-SCT is being quenched or blown

out. Figures 28 and 29 show the inversion of the emission characteristics at all but mode 5. The likely cause of this is excessive EGR, due to the added restriction of the modified exhaust runners. While the UIdaho currently lacks the ability to measure EGR, oxides of nitrogen (NO_x) emissions can offer some clues about the presence of EGR. NO_x emissions are heavily temperature dependent, with NO_x formation essentially becoming stopping below 2250K. [2] EGR reduces combustion flame temperatures, with five to ten percent EGR reducing to reduce NO_x by half. [16] When looking at the NO_x emissions, the PR-SCT appears to have about half the NO_x emissions as the stock engine. However, the measured NO_x at these points is within the error of the measurement. These lower temperatures would prevent the combustion of the fuel, leaving mostly HC emissions and preventing the formation of CO.

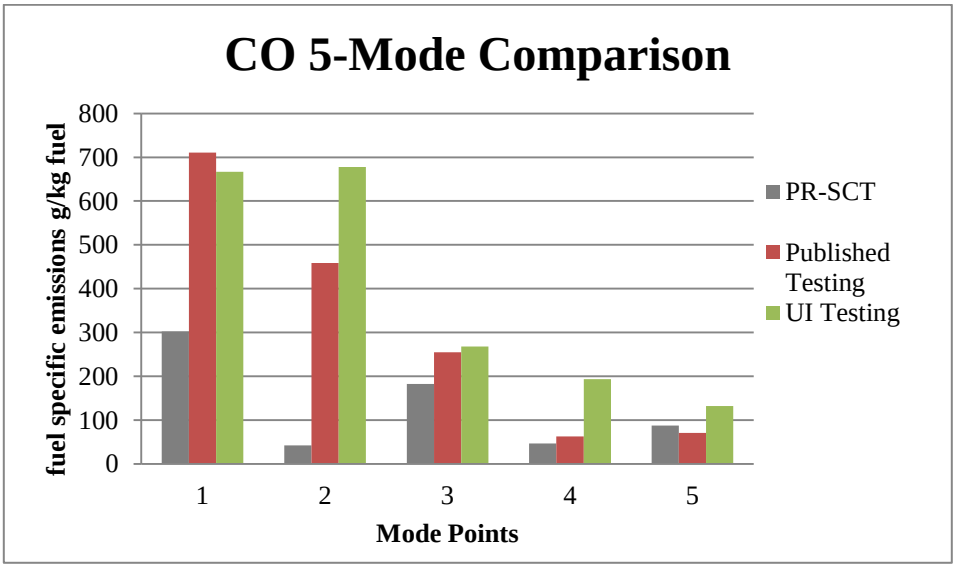

Figure 28: EPA 5-Mode CO Comparison [12]

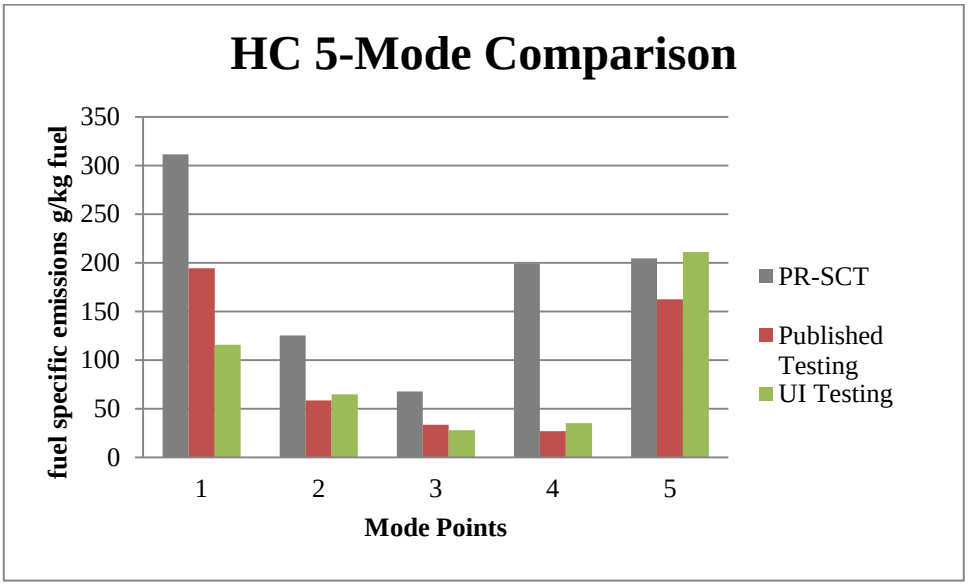

Figure 29: EPA 5-Mode HC Comparison [12]

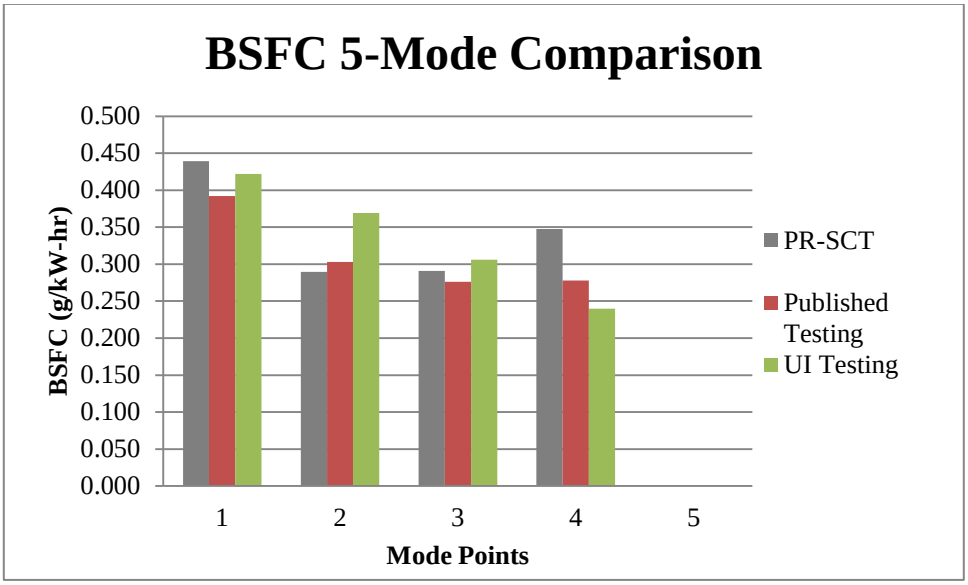

Figure 30: EPA 5-Mode BSFC Comparison [12]

While the PR-SCT appears to suffer from incomplete combustion, looking at BSFC, the PR-SCT is competitive with the stock engine. The PR-SCT, on average, had BSFC values 5% larger than the stock engine. Modes 2 and 4 are outliers of this trend, as mode 2 surpassed

the stock engine by approximately 5% and mode 4 was approximately 25% higher than the stock engine.

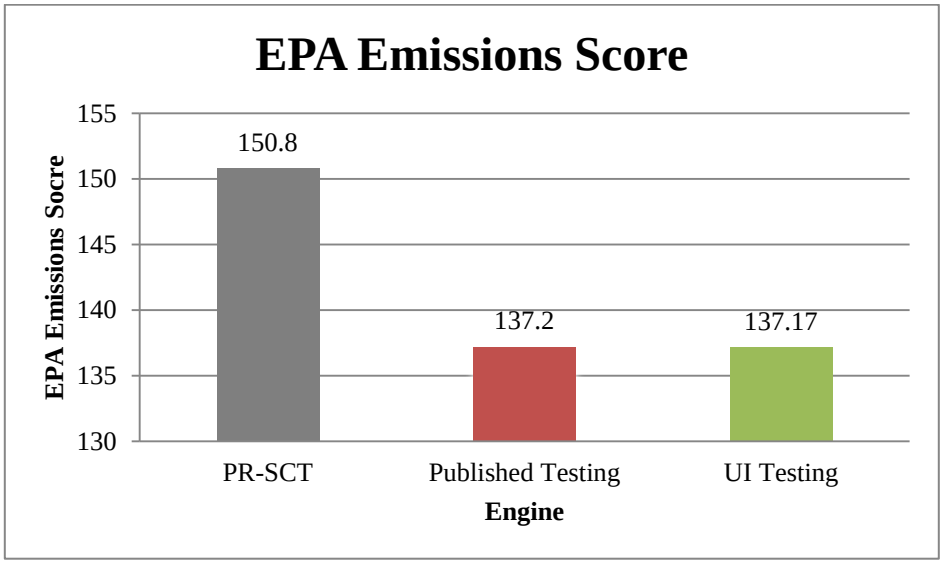

Figure 31: EPA Emissions Score Comparison [12]

Looking at the total emissions score, the PR-SCT performance surpasses the stock engine. This was unexpected since the PR-SCT appears to suffer from incomplete combustion. Reductions in incomplete combustion would likely make the engine capable of passing NPS standards. An important note is, while the different testing of the stock engine had different HC and CO values at each mode, the total emissions score was nearly identical.

7 Conclusions

7.0 Incomplete combustion

While the PR-SCT was able to compete with stock engine, its performance appears to suffer from incomplete combustion due to excessive EGR. After talking with an engineer in the two-stroke engine industry, the likely cause of the EGR is due to its large exhaust runner volume required for the valve's area of travel. [17] Initially, it was thought that excessive squish velocities were blowing out the flame. But, after measuring the PR-SCT engine, its squish velocities were found to be only slightly higher, and with no limitations on squish velocity, this was determined not to be the cause. [17] Table 7 shows the difference in the squish velocities of the PR-SCT and stock engine at different test points.

	Mode 5 1200 RPM	Mode 4 4050 RPM	Mode 3 4700 RPM	Mode 2 5350 RPM	Mode 1 6300 RPM	Hooper 5200 RPM
Stock	4.676 m/s	15.78 m/s	18.32 m/s	20.85 m/s	24.55 m/s	20.26 m/s
PR-SCT	5.266 m/s	17.77 m/s	20.63 m/s	23.48 m/s	27.65 m/s	22.82 m/s

Table 7: Squish Velocities at different RPMs

7.1 Optimum Valve Angle

While the exact optimum VA is not able to be determined at most mode points, it can be accurately determined within 10°. Looking at the VA sweeps, it appears relatively small to no changes in VA are needed until engine speed approaches 6000 RPM. This change is required at approximately 6000 RPM, as the tuned pipe is beginning to take effect and requires the valve to be less obstructive of EG flow. Different optimum VAs for each mode

point may prove worthwhile, but the use of the UIdaho's new California Analytical Instruments emissions analyzer would be required to reduce the error in trapping efficiency and exhaust emissions to determine these values.

7.2 PR-SCT Viability

The new valve face proved to provide a large improvement over the previous design**.** Drastically reducing exhaust emissions, compared to Hooper's PR-SCT, while providing improvements in BSFC and BMEP. These improvements brought the PR-SCT close to performance and exhaust emissions of the stock engine at its mode 4. The PR-SCT was also able to complete an EPA 5 mode emissions test, using the maximum engine speed of 6300 and maximum horsepower of 60 Hp. Comparing this power value to the stock engine at the same engine speed, the stock engine produces approximately 75 Hp. [18] Though it fails to produce the same power as the stock engine, it was able to nearly match the BSFC of the stock engine, while surpassing the stock engine's emissions score. The emissions score of the PR-SCT would likely increase with reduction of HC emissions. As shown in Figure 29 HC emissions are significantly larger than the stock engine, showing promise of an increased emissions score with reduction of HC emissions caused by incomplete combustion. The emissions score is currently as high as it is due low CO emissions from incomplete combustion. As reductions in incomplete combustion happen the CO emissions will increase and the emissions score will decrease. All of the above results show that the PR-SCT engine is still a worthwhile and viable research area. While further improvements are recommend in its design and tuning, it may prove to be successful in meeting its original design goals.

8 Suggested Future Work

8.0 Combustion Analyzer

To better help determine the combustion characteristics of the PR-SCT, the UIdaho combustion analyzer should be utilized to measure in-cylinder pressure traces. An encoder needs be added to the PR-SCT crankshaft to accurately measure crankshaft position, to assist in analyzing the pressure traces. The combustion analyzer will allow for the mass fraction burned to be calculated, to help determine optimum calibration points.

8.1 Electronic Valve Adjustment

The adjustment of the PR-SCT valve position needs to be electronically controlled for the PR-SCT engine to continue development. Current methods of manually adjusting position work for basic testing, but are time intensive. Electronic adjustment would reduce the calibration time required and, more importantly, allow VA adjustment while the engine is running. If the PR-SCT engine is to ever make it into a snowmobile chassis, electronic valve adjustment on the fly will be required for the engine to be successful and should be attempted with the next iteration of development.

8.2 Redesign of Pulley System

The pulley system has always been a concern with the PR-SCT engine. The latest iteration provided improvements in reliability, wear, and valve speed oscillation. However, it was not without failure. Excessive load was placed on the valve shaft pulley from belt tension. This caused the interior diameter of the pulley to become worn, along with failure of the pulley's set screws. On top of this, failure of the bearings in the pulley support bracket, mounted on the engine, case occurs. The valve shaft diameter was worn severely at the bearing locations.

Another issue with the pulley system is, when belt tension is applied, both pulley arms twist, causing belt misalignment and bearing wear in the pulley arms. A new pulley system should be designed, utilizing a new pulley support bracket that can support a larger valve shaft bearing, and is free of deflection. New pulley arms should be designed that are torsionally stronger; Plus, another method should be used for fixing the valve shaft pulley to the valve shaft, instead of two set screws. A custom valve shaft with varying diameters may be required for the valve shaft not to fail. The valve shaft should have a larger diameter before the cylinder, tapering off as reaches the cylinder bearings with the minimum diameter being the current valve shaft diameter.

8.3 Exhaust Valve Redesign

The exhaust flow of the PR-SCT engine is too restrictive for the engine to properly function. The valve face should be redesigned to have a shorter valve face, meaning the valve is capable of blocking off less of the exhaust port height. When the valve is rotating out of the way, it is partially blocking off the exhaust flow during scavenging. If the valve were smaller, less restriction should be present, and the scavenging efficiency of the engine may increase. An added benefit of the smaller valve design is less stress on the valve shaft. Failure of the valve shaft ultimately led to end of testing of the PR-SCT. Plastic torsional deformation led to the valve shaft failing at the pins holding counter weights in place at the mag side cylinder. These pin locations were stress concentration points on the valve shaft, with the shaft deforming approximately 45° counterclockwise before failure. The broken valve shaft and valve can be seen in Figure 32. The deformation at the pin locations can be easily seen, as it should be parallel to the pin locations on the valve.

Figure 32: Mag Side Valve After Failure

8.4 Exhaust Runner Redesign

Another area of improvement for exhaust flow is the exhaust runner area. The large volume in the exhaust runner is needed for valve movement, but is likely causing flow path issues. The large volume is also likely causing increased back pressure, which does not allow the pipe to effectively create a negative pressure wave. [17] A new exhaust runner area should be developed using CFD modeling to remove as much restriction as possible and reduce the exhaust runner volume. This should help increase scavenging efficiency, along with the maximum engine speed, as the exhaust runners are the largest source of restriction currently.

9 Bibliography

[1] Agster, "Principle of a tuned pipe for two-stoke engines," 2003. [Online]. Available: <http://www.schwabenkart.de>. [Accessed 24 August 2013].

[2] J. B. Heywood and E. Sher, The Two-stroke Cycle Engine, Philadelphia: Taylor & Francis, 1999.

[3] A. Hooper, "Comparision of Synchronous Charge Trapping and Variable Exhaust Valves in a Two-Stroke Engine," University of Idaho, Master's Thesis, Moscow, 2013.

[4] D. Dixon, "Comparison of Variable Exhaust Flow Techniques in a Modern Two-Stroke Engine," University of Idaho, Master's Thesis, Moscow, 2012.

[5] J. Johnson, "Comparison of Stratified and Homogeneous Combustion in a Direct-injected Two-stroke Engine for Snowmobile Applications," University of Idaho, Master's Thesis, Moscow, 2007.

[6] N. Bradbury, "Retrofitting Direct-Injection and a Turbocharger to a Two-Stroke Engine for Snowmobile Application," University of Idaho, Master's Thesis, Moscow, 2006.

[7] P. Britanyak, "Synchronous Charge Trapping Modification of a Two-Stroke Engine," University of Idaho, Master's Thesis, Moscow, 2010.

[8] A. Fuhrman, A. Hooper, T. Lord and C. Bode, ""Synchronous Charge Trapping Final

Report"," Not yet published, Moscow, 2011.

[9] G. P. Blair, Design and Simulation of Two-Stroke Engines, Warrendale, PA: Society of Automotive Engineers, 1996.

[10] R. Douglas, "AFR and Emissions Calculations for Two-Stroke Cycle Engines," Society of Automotive Engineers, 1990.

[11] A. Hooper, Interviewee, *Personal Correspondence.* [Interview]. July 2013.

[12] S. Miers, C. Green, J. Meldrum, C. Lundberg, W. Silvis and H. Pankratz, "Measurement of Dry Soot and Particulate Matter from Two-Stroke and Four-Stroke Snowmobiles," Society of Automotive Engineers, 2010.

[13] B. &. S. SRL, Eddy Current Dynamometer Instruction Manuel, Bologna: Italy, 1998.

[14] A. Welch, "Performance and Emissions Analysis of a Synchronous Charge Trapped Two-Stroke Engine," University of Idaho, Master's Thesis, Moscow, 2012.

[15] J. White and C. Wright, "Development and Validation of a Snowmobile Engine Emissions Test Procedure," Society of Automotive Engineers, 1998.

[16] R. Stone, Introduction to Internal Combustion Engines, Chippenham: Macmillan Press, 1999.

[17] R. Hays, Interviewee, *Personal Correspondence.* [Interview]. 27th September 2013.

[18] D. T. Research, "Ski-doo 2009 E-TEC Demonstrator Sled," 23 March 2008. [Online]. Available: http://www.dynotechresearch.com/file_upload/page_files/DTRETECBilly.pdf. [Accessed 2 October 2013].

[19] M. Nuti, Emissions From Two-Stroke Engines, Warrendale: Society of Automotive Engineers, 1998.